Self-consistent elastic continuum theory of degenerate, equilibrium aperiodic solids

Dmytro Bevzenko
Department of Chemistry, University of Houston, Houston, TX 77204-5003
Vassiliy Lubchenko[a)]
Department of Chemistry, University of Houston, Houston, TX 77204-5003 and
Department of Physics, University of Houston, Houston, TX 77204-5005

(Dated: 21 October 2014)

We show that the vibrational response of a glassy liquid at finite frequencies can be described by continuum mechanics despite the vast degeneracy of the vibrational ground state; standard continuum elasticity assumes a unique ground state. The effective elastic constants are determined by the bare elastic constants of individual free energy minima of the liquid, the magnitude of built-in stress, and temperature, analogously to how the dielectric response of a polar liquid is determined by the dipole moment of the constituent molecules and temperature. In contrast with the dielectric constant—which is enhanced by adding polar molecules to the system—the elastic constants are down-renormalized by the relaxation of the built-in stress. The renormalization flow of the elastic constants has three fixed points, two of which are trivial and correspond to the uniform liquid state and an infinitely compressible solid respectively. There is also a nontrivial fixed point at the Poisson ratio equal to 1/5, which corresponds to an isospin-like degeneracy between shear and uniform deformation. The present description predicts a discontinuous jump in the (finite frequency) shear modulus at the crossover from collisional to activated transport, consistent with the RFOT theory.

arXiv:1409.7357v2 [cond-mat.dis-nn] 20 Oct 2014

I. INTRODUCTION

In the absence of kinetic access to a crystalline or partially ordered state, a liquid can be equilibrated even below the fusion temperature. If such a liquid is sufficiently pressurized and/or cooled, it undergoes a crossover from largely collisional to activated transport,[1,2] whereby long-lived aperiodic structures begin to form; these can be seen directly by neutron scattering.[3] The crossover is manifested thermodynamically as a breaking of the translational symmetry upon which the particle density profile is no longer uniform but consists of disparate, narrow peaks.[4] For example, in ordinary, chemically-bonded liquids the crossover takes place at viscosity values around 10 Ps or, equivalently, when the α-relaxation time is about three orders of magnitude longer than the vibrational relaxation time: $\tau_\alpha \simeq 10^3 \tau_{\rm vibr}$.[1,5] The crossover to activated transport can occur either below or above the fusion temperature, depending on the liquid's fragility.[1] In the latter case, the liquid is technically supercooled. For generality, we will use the term "glassy" for a liquid below the crossover—but above the glass transition—since the glass transition is always preceded by the crossover in ordinary liquids.

As worked out in the random first order transition (RFOT) theory, particles move below the crossover via local activated reconfigurations between distinct aperiodic free energy minima,[6,7] see Ref. 8 for a review. These reconfigurations are responsible for the α-relaxation. They involve several hundred atoms near the glass transition; the corresponding cooperativity length scale ξ is numerically $2-4$ nm in actual substances,[7,9] consistent with observation.[10–13] The cooperative reconfigurations are driven by the multiplicity of the distinct aperiodic free-energy minima, whose log-number is called the configurational entropy. The configurational entropy is inherently connected and numerically close to the excess liquid entropy relative to the corresponding crystal; this excess entropy can be inferred from experiment.[14,15]

The activated reconfigurations restore the ergodicity and dictate that the zero-frequency modulus be zero. Despite this liquid-like response at the very lowest frequencies, the material exhibits *elastic* response at nonzero frequencies. The vibrational response of supercooled liquids, at these frequencies, apparently obeys standard continuum mechanics and can be measured, for instance, by Brillouin scattering.[5] Yet continuum mechanics assumes at the onset that there is a unique vibrational ground state. Under this assumption, the particle identities in the ground state and in a vibrationally excited state can be strictly matched thus allowing one to define local displacement $\mathbf{u}$ unambiguously. In contrast, a liquid in the activated transport regime—as it would be near its glass transition—is a mosaic of aperiodic structures each corresponding locally to distinct, individual minima of the free energy;[7] the built-in stress at the physical boundaries between the structures, due to the mutual mismatch, cannot be removed by elastic deformation. While vibrational excitations within individual minima are well defined, this is not so for the actual liquid, because the structure relaxes on a finite time scale. In fact, a liquid of volume V will experience local relaxation roughly once per time $\tau_\alpha \xi^3/V$.[16] Thus the larger the region, in which one considers vibrational excitations such as sound waves, the more ambiguous it is to define a vibrational ground state.

[a)] vas@uh.edu

Here we determine the vibrational response of such an equilibrium, degenerate aperiodic solid starting from the elastic properties of *individual* aperiodic free energy minima. We show that the question is in many ways analogous to the problem of determination of the dielectric response of a fluid given the dipole moment and polarizability of the constituent molecules.[17–20] The role of the permanent dipoles is played here by the built-in mechanical stress, a tensorial quantity. Even when mechanically stable, all solids are inherently stressed:[21] For instance, in a bulk periodic crystal, the bond lengths differ from their values in very small clusters made of the same material. Crystal surfaces are often reconstructed.[22,23] These are rather trivial examples in that the stress can be removed by deformation without breaking bonds; this simple kind of stress not classified as built-in. Much more interesting are strains arising in the presence of vacancies/interstitials, dislocations, or disclinations. These sources of strain *cannot* be removed without breaking bonds. A simple but key signature of built-in stress that it cannot have an arbitrarily small magnitude; the magnitude must be *finite*. Conversely, stress of arbitrarily small magnitude can be removed by elastic deformation.

In glassy solids, local stresses are mutually frustrating and lead to structural *degeneracy*, which is manifested thermodynamically as the configurational entropy, as mentioned. The concentration of the stressed regions is inherently $1/\xi^3$, where ξ is the volumetric size of the cooperatively rearranging region during α-relaxation. A similar example of such frustration constructed theoretically is that arising in icosahedral order;[24] the corresponding free energy landscape is consistent with the predictions of the RFOT theory.[25] Inherent stresses arising in solids owing to aperiodicity have been discussed previously in Refs. 26–28.

The picture of a supercooled liquid as a stressed degenerate continuum emerges in the analysis by the present authors[29] (BL), which is complementary to the RFOT theory in that it considers a non-degenerate, stable solid—not the uniform liquid—as the reference state for building the glassy state. (Presumably, such a non-degenerate solid is ordinarily periodic in 3D.) In the BL construct, one splits the total deformation tensor:[30]

$$\varepsilon_{ij} \equiv \frac{1}{2}\left(\frac{\partial u_i}{\partial x_j} + \frac{\partial u_j}{\partial x_i}\right) \equiv \frac{1}{2}\left(u_{i,j} + u_{j,i}\right) \qquad (1)$$

into a sum of a small-k (long-wavelength) contribution $\varepsilon^<_{ij}$ and large-k (short-wavelength) contribution $\varepsilon^>_{ij}$: $\varepsilon_{ij} = \varepsilon^<_{ij} + \varepsilon^>_{ij}$. Upon denoting the short-wavelength part as $\eta_{ij} \equiv \varepsilon^>_{ij}$, the usual vibrational free energy[30] reads:

$$\mathcal{F} = \frac{1}{2}\int \mathrm{d}V \left(\boldsymbol{\varepsilon}^< + \boldsymbol{\eta}\right) \mathsf{C}_0 \left(\boldsymbol{\varepsilon}^< + \boldsymbol{\eta}\right), \qquad (2)$$

where C_0 is the elastic moduli tensor. Subsequently, one fixes the magnitude of the short-wavelength stress:

$$\boldsymbol{\eta}(\mathbf{r})\mathsf{C}_0\boldsymbol{\eta}(\mathbf{r}) = g^2(\mathbf{r}). \qquad (3)$$

thus (artificially) making it built-in. With this constraint, the simple model from Eq. (2) becomes strongly non-linear. We associate the lengthscale below which the stress cannot relax with the size a of the chemically-rigid molecular unit, or "bead."[1,29] Conversely, the elastic degrees of freedom $\varepsilon^<_{ij}$ are essentially phonons with $k < \pi/a$.

We have shown that given a large enough magnitude g of built-in stress, there emerges self-consistently a metastable, structurally-degenerate aperiodic state separated by a nucleation barrier from the stable, unique reference state. In the simplest treatment, one finds that the structural degeneracy of a supercooled liquid maps onto the set of mutual orientations of an assembly of six-component Heisenberg spins on a fixed lattice with anisotropic interactions. The six components reflect the number of independent entries of the deformation tensor from Eq. (1). One can make parallels between the BL picture and that by Yan et al.[31], in whose model the degeneracy is built-in by assuming individual bonds can switch between two alternative lengths, where the switching is controlled by an Ising-like variable.

In terms of the aforementioned analogy with the dielectric response, the *stable* vibrational ground state—i.e., elastic medium without built-in stress—corresponds to vacuum, while the sources of stress correspond to molecular dipoles. As in the dielectric case, the interaction between the sources of stress scales with the distance r as $1/r^3$, although it is now of more complicated, tensorial form.

There are several, distinct motivations for the present calculation. The most immediate motivation is to connect the characteristics of local stress to the elastic properties of the solid, much like Onsager determined the dielectric response of a liquid using the dipole moment and polarizability of individual molecules as the microscopic input. To quantify the renormalization of the elastic moduli—and especially their decrease upon approaching the cross-over from below—is essential for building a theory of the glass transition.[31–33]

A distinct motivation is to accomplish the BL programme of detailed characterization of the activated dynamics in liquids via the 6-component spin model, which has certain advantages over direct simulation of liquids: The spins are not subject to collisional effects that represent a significant source of slowing down in liquid simulations. The spin model has a significantly smaller number of degrees of freedom than the corresponding liquid since the purely vibrational modes $\boldsymbol{\varepsilon}$ can be integrated out. In addition, the spins are situated on a *fixed* lattice, making it easier to define an order parameter for activated reconfigurations, so that configurations can be distinguished based on the orientations of the 6-spins. An explicit advantage of the elasticity-based approach of BL is that the complicated inter-atomic forces enter the description only through very few parameters. In the most minimal description, this set of parameters includes only the compressibility, shear modulus, and bead size. Conversely, the explicit functional form of the many-body forces in

actual materials is simply unavailable even though simplified, effective potentials, such as the BKS model[34] of amorphous silica, have been reasonably successful in reproducing several material properties. Incidentally, direct simulations of actual liquids still remain excessively computationally costly. Only for simple systems, such as Lennard-Jones or hard sphere mixtures, the onset of activated transport seems to have been reached in simulation, see Ref. 35 and references therein.

One of the most challenging aspects of the BL program is that the spin-spin interaction scales as $1/r^3$ and thus is much longer-range than ordinary molecular interactions; this potentially leads to artifacts in simulations due to finite-size effects. For instance, imposing periodic boundary conditions on models with such long-range interactions will likely produce excessive finite-size effects. Indeed, simulations of dipolar systems on periodic lattices have produced ordered states.[36] To avoid such artifacts, one may employ a different type of boundary conditions, in which the spins inside a compact region are treated explicitly, while the outside spins are approximated as an elastic continuum. This is in direct analogy with the Onsager cavity construction,[17] except here one treats the number of particles inside the cavity as a flexible parameter; the Onsager limit is achieved in the limit of one spin per cavity. The cavity construction is often used in computer simulations of polar liquids.[37] Additionally, imposing the self-consistency in the determination of the elastic response lends further support to the BL picture, as the latter is not fully self-contained: The stabilization of the aperiodic phase stemming from steric repulsion, mentioned earlier, is not explicitly treated in the present version of the BL formalism, but is assumed. Finally, achieving the self-consistency using a continuum treatment alleviates concerns about the ultraviolet behavior of the BL model, in which local sources of built-in stress are approximated as point-like objects, while their mutual spacing enters through the ultraviolet cut-off in phonon sums.

Last, but not least, this work addresses the fundamental challenge of developing continuum mechanics for a medium that has a vastly degenerate ground state. Ordinary theory of elasticity[30] simply assumes a unique reference state exists. All excitations in the latter theory are diffeomorphisms, i.e., combinations of stretches and contractions. The resulting states are all equivalent from the viewpoint of differential geometry since they have the same connectivity. In chemical language, no bonds can be broken or made during such elastic deformation. The above notions can be formalized as follows. The energy of an elastic deformation can only depend on the spatial *derivative* of the actual atomic displacement $\mathbf{u}$ since this energy does not depend on the absolute location of the body in space. Thus in the lowest order, the deformation is described by a (symmetric) tensor from Eq. (1) which has six independent components and thus potentially over-defines the actual particle displacement, which has only three independent components. The conventional continuum mechanics adopts a specific condition on the ε_{ij} tensor that turns out to supply exactly three constraints. This condition insures that the integration of the deformation tensor ε_{ij}—with the aim of computing the actual displacement $\mathbf{u}$—gives the same result regardless of the contour of integration. In chemical language, this is equivalent to requiring that no bonds are broken during deformations. By the Saint-Venant theorem, see e.g. Ref. 38, this can be achieved, if the so called "incompatibility" tensor is identically zero:

$$\left(\mathrm{inc}\,\boldsymbol{\varepsilon}\right)_{ij} \equiv -\epsilon_{ikl}\epsilon_{jmn}\varepsilon_{ln,\,km} = 0, \tag{4}$$

where ϵ_{ijk} is the Levi-Civita symbol. Throughout, we imply summation with respect to doubly-repeated indices. Given a deformation tensor ε_{ij} that satisfies constraint (4), the atomic displacement $\mathbf{u}$ can be unambiguously computed using the Kirchhoff-Cesàro-Volterra formula.[38,39] Condition (4) is analogous to the constraint one imposes in electrodynamics (in the absence of charges) that the electric field be rotor-free: $\boldsymbol{\nabla}\times\mathbf{E}=0$. Only under such circumstances can the electric field be expressed as the gradient of a single-valued, scalar field; this is needed to make the energy of an electric charge subject to electric field a well defined, single-valued function of the coordinate. Note that the existence of a unique reference state for the continuum mechanics is analogous to stipulating that vacuum be unique in electrodynamics.

The differential-geometric formulation of continuum mechanics[40] generalizes the defect-free description corresponding to Eq. (4) to more complicated situations when dislocations and vacancies/interstitials are present, by introducing *torsion* and *nonmetricity* respectively. Thus one tacitly assumes there is an underlying Bravais lattice in the continuous description. Applicability of such description to glassy systems is far from certain however. On the one hand, there is no underlying Bravais lattice in a supercooled liquid or glass. At the same time, the coordination varies spatially. Consequently, describing the space itself, let alone potential defects in the space, by continuum methods becomes ambiguous. Generally, defining defects in a disordered medium is ambiguous, too: As emphasized in Refs. 41–44, supercooled liquids or glasses cannot be regarded as defected versions of crystal since the crystal portion of the phase space is not accessible to the system. Consistent with these notions, Cammarota and Biroli[45] argued there is no static pattern corresponding to the metastability of a supercooled liquid with respect to local reconfiguration between alternative free energy minima. Thus the lengthscale corresponding to those stress patterns generally must be—and has been[10–13]—determined dynamically. It is not clear at present whether the local free energy excess due to built-in *stress* in glassy liquids can be measured by linear spectroscopy. Still, note that in one family of glasses, viz. chalcogenide alloys, the stressed regions have an electronic signature in the form of midgap electronic states[42,44] that can be detected by

essentially linear means.[46,47] In addition, the amount of built-in stress may be modified by varying the speed of quenching or as a result of polymerization below the glass transition, leading to a change in vibrational properties of the glass.[48]

The notions of the structural degeneracy and the resulting steady structural reconfiguration between alternative aperiodic structures are key to the present work. A fully *stable* lattice—periodic or aperiodic—has a unique vibrational ground state, in contrast with actual glassy liquids that are prevented from crystallization. Even though plane waves are no longer vibrational eigenmodes in a stable aperiodic lattice, there is no ambiguity in defining an elastic response down to zero frequencies. Far from simple, the vibrational response of stable aperiodic lattices generally includes non-affine displacements,[49] which *also* violate the Saint-Venant compatibility condition (4).[50] Local elastic response in aperiodic lattices is generally spatially inhomogeneous;[28,51,52] the distribution has been argued to cause down-renormalization of the bulk elastic constants.[53,54]

The present theory of elasticity of equilibrium aperiodic solids, such as supercooled liquids, is based on the notions of structural degeneracy and built-in stress, not structural inhomogeneity per se. The article works out the resulting microscopic picture in the following logical sequence: In Section II, we briefly review the theory of dielectrics, which relates the expectation value of local polarization to the bulk dielectric response of the material. There we also review Onsager's construction for determining the local polarization and the effective dielectric constant of the liquid self-consistently, based on the dipole moment of individual molecules. Section III demonstrates that the type of uniformly distributed built-in stress characteristic of glassy liquids is analogous in several ways to molecular dipoles in an equilibrated fluid. Alongside, the analogy between continuum electrodynamics and mechanics is explained and elements of tensor algebra that greatly facilitate the analysis of the elastic case are reviewed. In Section IV, we make a connection between the expectation value of the built-in stress and renormalization of the elastic constants. In Section V, we compute the interaction between local sources of built-in stress, which is the analog of the dipole-dipole interaction in electrodynamics. Section VI works out the generalized cavity construction for elasticity. We obtain formal expressions for the vibrational response of a degenerate, equilibrium aperiodic solid, in which a compact subset of local sources of built-in stress are treated explicitly while its environment is approximated as an elastic continuum with effective elastic constants. Section VII determines the bulk elastic response of such a solid approximately for three specific implementations of the built-in stress. In all cases, the elastic constants are *down*-renormalized owing to the built-in stress in contrast with the dielectric case, in which the dielectric constant can only be enhanced by molecular dipoles. In addition to the trivial fixed points to the elastic renormalization—which correspond to the uniform liquid and infinitely compressible solid—a special value of the Poisson ratio, $\nu = 1/5$, emerges as a non-trivial fixed point that corresponds to a special degeneracy between pure uniform and shear deformations.

The first implementation of the built-in stress is closest in spirit to the Onsager approximation and amounts to a source of built-in stress directly in contact with the effective elastic medium. We establish that there is a limiting value to the built-in stress past which the mechanical stability limit of the aperiodic solid is reached. We also find self-consistently that a uniform liquid cannot sustain built-in stress. The second implementation is appropriate for realization of the BL program in which an arbitrarily large, compact subset of the sources are treated explicitly while the environment is approximated as an elastic continuum. The third implementation is a systematically worked-out analog of how the built-in stress was set up in the original BL paper.[29] Here we find that the $\nu = 1/5$ fixed point is *repulsive*, in contrast with the first two cases. This repulsive fixed point is consistent with the critical point at $\nu = 1/5$ found in the mean-field limit of the BL model. The corresponding continuous transition separates two relatively distinct regimes in which a supercooled liquid can be viewed as a frozen-in stress pattern corresponding to largely uniform dilation/compression and shear respectively. In all three implementations, we observe that the transition between the uniform liquid and the degenerate, aperiodic crystal is discontinuous, consistent with the RFOT theory. In the final Section VIII, we discuss and summarize the present findings.

II. REVIEW OF THE CAVITY CONSTRUCTION FOR POLAR LIQUIDS

The present argument for determination of the mechanical response of an aperiodic solid, as a degenerate collection of sources of stress, is relatively complex mathematically, partially because of the tensorial character of mechanical deformation. It seems most profitable to present this argument by analogy with the simpler calculation of the dielectric response of polar liquids, which are characterized by a multiplicity of distinct configurations of the molecular dipoles.

Consider a dielectric liquid with susceptibility ϵ and assume that chemically inert, polar molecules are dissolved in the liquid at a low concentration c. We label the magnitude of the permanent dipole moment of the solute molecules by d and neglect their polarizability, since we will not be considering the elastic analog of the polarizability in what follows. ("Elastic polarizability" is usually neglected in treatments of elastic defects.[55–57]) Our task is to determine the effective dielectric constant ϵ' of the solution self-consistently. Note we set up the dielectric problem a bit differently from the conventional procedure, which fixes the bare dielectric susceptibility

in the absence of solute at its value in vacuum, whereby $\epsilon = 1$.

By definition, the local value of the electric displacement in the solution is[58]

$$\mathbf{D} = \mathbf{E} + 4\pi \left(\mathbf{P}^{\mathrm{B}} + \mathbf{P}^{\mathrm{D}}\right), \tag{5}$$

where $\mathbf{E}$ is the local value of the electric field and the total polarization is the sum of two components: the polarization $\mathbf{P}^{\mathrm{B}}$ of the bare solvent and the polarization $\mathbf{P}^{\mathrm{D}}$ of the solute. Since the dependence of $\mathbf{P}^{\mathrm{B}}$ on the electric field is known, $(\epsilon - 1)\,\mathbf{E} = 4\pi\mathbf{P}^{\mathrm{B}}$, it can be excluded from Eq. (5) to yield

$$\mathbf{D} = \epsilon\mathbf{E} + 4\pi\mathbf{P}^{\mathrm{D}}. \tag{6}$$

The total dielectric constant ϵ' of the solution can be defined as the proportionality coefficient between the volume averages of $\mathbf{E}$ and $\mathbf{D}$, similarly to how the effective dielectric constant of a mixture is defined,[58]

$$\overline{\mathbf{D}} = \epsilon'\,\overline{\mathbf{E}} \qquad \text{or} \qquad \epsilon'\,\overline{\mathbf{E}} = \epsilon\overline{\mathbf{E}} + 4\pi\overline{\mathbf{P}}^{\mathrm{D}}, \tag{7}$$

where the averaging is done over a volume containing an appreciable number of solute molecules. As suggested by Eq. (7), $\overline{\mathbf{P}}^{\mathrm{D}}$ is a function of the mean field $\overline{\mathbf{E}}$ only. In the linear-response regime, we obtain

$$\overline{P}_i^{\mathrm{D}} = \chi_{ij}\overline{E}_j, \tag{8}$$

where

$$\chi_{ij} \equiv \left.\frac{\partial \overline{P}_i^{\mathrm{D}}}{\partial \overline{E}_j}\right|_{\overline{\mathbf{E}}=0} \tag{9}$$

is the static isothermal response function of the solute as dissolved in the solvent. We have used that in equilibrium, $\overline{\mathbf{P}}^{\mathrm{D}} = 0$ in the absence of external field. Substituting Eq. (8) into Eq. (7) one obtains the following relation between the bare and effective dielectric constants:

$$\epsilon' = \epsilon\delta_{ij} + 4\pi\chi_{ij}. \tag{10}$$

To calculate the susceptibility χ_{ij} we must use a specific model for dipole dynamics in the solution. At high temperatures, a good approximation is afforded by the Onsager cavity construction.[17] Assuming the solute concentration is c, the polarization density is, approximately,

$$\overline{\mathbf{P}}^{\mathrm{D}} \approx c\langle\mathbf{d}\rangle, \tag{11}$$

where $\langle\mathbf{d}\rangle$ is the thermally averaged value of an individual molecular dipole. We treat an individual, chosen molecular dipole explicitly while approximating the response of the rest of the dipoles to the motions of the chosen dipole by the response of a dielectric continuum with an effective dielectric constant ϵ'. The chosen dipole is placed, by construction, in the center of a spherical cavity of radius $r_0 = (3/4\pi c)^{1/3}$. The medium inside the cavity is still characterized by the bare dielectric constant ϵ.

The inhomogeneity in the local dielectric response due to the cavity does not, on average, modify the electric displacement $\mathbf{D}$, since the latter is determined by the charge distribution *outside* the sample. We assume, in a mean-field fashion, that the displacement is in fact spatially homogeneous: $\mathbf{D} = \overline{\mathbf{D}}$. Consequently, the electric field far away from the cavity is also homogeneous and, by Eq. (7), is equal to the mean field $\overline{\mathbf{E}}$,

$$\mathbf{E} = \mathbf{D}/\epsilon' = \overline{\mathbf{E}}. \tag{12}$$

The resulting electric field inside the cavity can be computed in a standard fashion:[59]

$$\mathbf{F} = \frac{3\epsilon'}{2\epsilon' + \epsilon}\overline{\mathbf{E}} + \frac{2\left(\epsilon' - \epsilon\right)}{a^3\epsilon\left(2\epsilon' + \epsilon\right)}\mathbf{d}, \tag{13}$$

where the first term on the r.h.s. gives the field $\overline{\mathbf{E}}$ modified by the dielectric discontinuity at the cavity-solvent interface while the second term is the image field of the dipole due to polarization at the interface. The potential energy of the dipole subsequently reads

$$\mathcal{E} = -\mathbf{d}\mathbf{F} = -\frac{3\epsilon'}{2\epsilon' + \epsilon}\mathbf{d}\overline{\mathbf{E}} - \frac{2\left(\epsilon' - \epsilon\right)}{a^3\epsilon\left(2\epsilon' + \epsilon\right)}d^2. \tag{14}$$

We can now calculate the average dipole moment and, via Eq. (11) and (9), the susceptibility χ_{ij}. In the high temperature limit,[17]

$$\langle\mathbf{d}\rangle = \frac{\int \mathrm{d}\Omega\mathbf{d}e^{-\beta\mathcal{E}}}{\int \mathrm{d}\Omega e^{-\beta\mathcal{E}}} \approx \frac{d^2\beta\epsilon'}{2\epsilon' + \epsilon}\overline{\mathbf{E}}, \tag{15}$$

where the integration is over all possible orientations of $\mathbf{d}$ and $\mathrm{d}\Omega$ denotes an infinitesimal element of the corresponding solid angle. Note that the image field in Eq. (14) does not affect the orientation of the dipole. We thus obtain for the susceptibility

$$\begin{aligned}\chi_{ij} = \left.\frac{\partial \overline{P}_i^{\mathrm{D}}}{\partial \overline{E}_j}\right|_{\overline{\mathbf{E}}=0} &= \left.\frac{3c\beta\epsilon'}{2\epsilon' + \epsilon}\left[\langle d_i d_j\rangle - \langle d_i\rangle\langle d_j\rangle\right]\right|_{\overline{\mathbf{E}}=0} \\ &= \frac{c\beta d^2\epsilon'}{2\epsilon' + \epsilon}\delta_{ij},\end{aligned} \tag{16}$$

which, upon substitution into Eq. (10), produces the following relation between the bare and full dielectric constants,

$$\epsilon' = \epsilon + 4\pi c\beta d^2\frac{\epsilon'}{2\epsilon' + \epsilon}. \tag{17}$$

As a result,

$$\frac{\epsilon'}{\epsilon} = \frac{1}{4}\left(1 + \frac{b}{\epsilon} + \sqrt{\left(1 + \frac{b}{\epsilon}\right)^2 + 8}\right), \tag{18}$$

where

$$b \equiv 4\pi c\beta d^2. \tag{19}$$

Equation (18) yields Eq. (26) from Onsager's paper,[17] if we neglect the polarizability and set ϵ to unity.

In the above procedure, one integrates out local degrees of freedom to determine the bulk response of the material. It is thus possible to interpret the Onsager construction as a coarse-graining procedure. From this viewpoint, one may regard relation (18) as a *renormalization* of the dielectric response due to local dipolar sources. For infinitesimal values of the parameter b, the renormalization flow looks particularly simple:

$$\epsilon' = \epsilon + \frac{b}{3}, \tag{20}$$

Since b is positive, the "renormalization flow" has a single, "infinite-temperature plasma" fixed point at $\epsilon' \to \infty$, where the Coulomb interaction is completely screened. The physical reason for this up-renormalization of the dielectric response is that molecular dipoles are directed, on average, *along* the field thus screening the field locally.

III. THEORY OF ELASTICITY: ANALOGY WITH ELECTROSTATICS AND DIGRESSION ON NOTATION AND TENSOR ALGEBRA

E. Kröner[60] has pointed out analogies between equations of electrostatics and continuum mechanics. These analogies, which are summarized in Table I, do not amount to a full correspondence, nevertheless, which has to do with more than just the difference in the tensor ranks of the objects in the two theories. The most basic objects of electrostatics and continuum mechanics are electric charge density ρ and body force $\mathbf{f}$ respectively. The former is the divergence of a vector, while the latter of a tensor, viz.:

$$4\pi\rho = D_{i,i} \tag{21}$$

and

$$f_i = -\sigma_{ij,j}, \tag{22}$$

where $\mathbf{D}$ is the dielectric displacement and σ_{ij} the elastic stress tensor.

The material relation $\mathbf{D} = \epsilon\mathbf{E}$ in a dielectric corresponds to Hooke's law in elasticity: $\sigma_{ij} = \mathsf{C}_{ijkl}\varepsilon_{kl}$, so that the tensor ε_{ij} plays the role analogous to the electric field $\mathbf{E}$ while the rank-four tensor of elastic moduli C_{ijkl} is analogous to the dielectric susceptibility, which is generally a 2nd rank tensor. Here we assume an isotropic dielectric medium for simplicity, so that the dielectric susceptibility tensor is proportional to the unit matrix, effectively allowing us to regard ϵ simply as a scalar. In the case of isotropic elasticity, some simplification is *also* possible, to be discussed shortly; still, the elastic response will have to be written out explicitly as a rank-four tensor.

Of particular importance are expressions for the free energy; to write these down we must choose an appropriate ensemble. For instance, in electrostatics one may choose to work at fixed charge or fixed field.[58] The latter is more convenient in the present context as we probe the response of the material to externally imposed field. Likewise, it will be convenient to work at fixed deformation in the elastic case. The resulting expression for the free energy increments are:[30,58]

Electrostatics	Elasticity
E_i	ε_{ij}
D_i	σ_{ij}
$4\pi P_i$	ω_{ij}
ρ	f_i
$D_{i,i} = 4\pi\rho$	$\sigma_{ij,j} = -f_i$
$D_i = \epsilon E_i$	$\sigma_{ij} = \mathsf{C}_{ijkl}\varepsilon_{kl}$
$\rho = -P_{i,i}$	$f_i = \omega_{ij,j}$
$\mathrm{rot}\,\mathbf{E} = 0$	$\mathrm{inc}\,\boldsymbol{\varepsilon} = 0$
$dF = -\frac{1}{4\pi}\mathbf{D}d\mathbf{E}$	$dF = +\sigma_{ij}d\varepsilon_{ij}$

TABLE I. Analogy between electrostatics and linear elasticity. Here $\mathbf{E}$ and $\mathbf{D}$ are the electric field and displacement vectors respectively. $\mathbf{P}$ is the electric polarization, ρ electric charge density, ε_{ij} and σ_{ij} elastic strain and stress tensors respectively, $\mathbf{f}$ the body force, ω_{ij} the internal stress, ϵ the dielectric susceptibility, C_{ijlm} the elastic moduli tensor, and dF the free energy increment.

$$dF = -\frac{1}{4\pi}\mathbf{D}d\mathbf{E} \qquad \text{and} \qquad dF = +\sigma_{ij}d\varepsilon_{ij}. \tag{23}$$

We have deliberately emphasized the distinct signs in front of the two increments for they are ultimately responsible for the difference in how the response functions are renormalized in the two descriptions in the presence of non-removable dipole moments and sources of stress respectively. We shall see that the elastic deformation is *enhanced* by the presence of built-in stress, in contradistinction with electrostatics.

The internal, or "built-in" stress in glassy materials can be introduced analogously to how polarization is introduced in the electrodynamics of continuous media.[58] In charge neutral dielectrics, $\int \mathrm{d}V\rho(\mathbf{r}) = 0$, and, hence, ρ must be the divergence of a vector, $\rho = -P_{i,i}$, that vanishes outside the dielectric.[58] Similarly, the volume average of the built-in body force $\mathbf{f}(\mathbf{r})$ in glassy materials vanishes in the absence of an external load, $\int \mathbf{f}(\mathbf{r})\mathrm{d}V = 0$, and, of course, vanishes outside. Hence, the force $\mathbf{f}$ is also a divergence, but of a tensor, which we call $\omega_{ij,j}$:

$$f_i = \omega_{ij,j}. \tag{24}$$

ω_{ij} vanishes at the surface of a sample. The force on particles resulting from the built-in stress must be exactly balanced out by the restoring force of the lattice. By Eq. (22),

$$\sigma_{ij,j} + f_i = \left(\sigma_{ij} + \omega_{ij}\right)_{,j} = 0. \tag{25}$$

Thus, ω_{ij} is an internal (built-in) stress distribution characterizing the state of an amorphous structure similar to how polarization $\mathbf{P}$ characterizes the state of a dielectric

material. One can think of the deformation corresponding to the stress tensor $\sigma_{ij,j}$ as the response of the lattice to a defect in the form of built-in stress. This deformation is compatible, in the sense of Eq. (4), while the deformation corresponding to the built-in stress itself is not.

To simplify notations, in the following we shall employ Walpole's conventions.[61] In addition to using Einstein's repeated index convention for tensor multiplication, we will drop indexes in inner products altogether. For instance, we often write $\boldsymbol{\sigma} = \mathsf{AB}\boldsymbol{\varepsilon}$ instead of $\sigma_{ij} = \mathsf{A}_{ijkl}\mathsf{B}_{klpq}\varepsilon_{pq}$, and $\boldsymbol{\sigma}\boldsymbol{\varepsilon}$ instead of $\sigma_{ij}\varepsilon_{ij}$. To avoid confusion we use upright fonts to label tensors (both fourth- and second-rank) whenever their indexes are not written out explicitly. Second-rank tensors are always denoted by bold lower case Greek letters, while fourth-rank tensors are denoted by capital sans-serif letters. As usual, the bold upright serif font is reserved for 3-vectors. We use the corresponding italic fonts for tensor and vector components. Note, that some of the Greek letters are conventionally reserved for scalars. For instance, μ and κ label shear and bulk moduli, ν is the Poisson ratio, and $\beta \equiv (k_{\mathrm{B}}T)^{-1}$. We also use index notations to label spatial derivatives, e.g. the derivative $\partial\omega_{ij}/\partial x_k$ of a second-rank tensor field $\boldsymbol{\omega}(\mathbf{r})$ is denoted with $\omega_{ij,k}$.

Most of the rank-4 tensors to be used below are isotropic. For these, algebra can be greatly simplified in the following way.[61] Consider for instance the elastic moduli tensor C of an isotropic medium with Lamé coefficients λ and μ,

$$\mathsf{C}_{ijkl} = \lambda\delta_{ij}\delta_{kl} + \mu\left(\delta_{ik}\delta_{jl} + \delta_{il}\delta_{jk}\right). \tag{26}$$

Hereby the elastic energy density,[30]

$$e = \frac{1}{2}\varepsilon_{ij}\mathsf{C}_{ijkl}\varepsilon_{kl}, \tag{27}$$

contains the only two scalars one can form using the entries of the deformation tensor:[30]

$$e = \frac{\lambda}{2}\varepsilon_{ii}^2 + \mu\varepsilon_{ij}^2 = \frac{\kappa}{2}\varepsilon_{ii}^2 + \mu(\varepsilon_{ij} - \frac{1}{3}\delta_{ij}\varepsilon_{kk})^2, \tag{28}$$

where κ is the bulk modulus:

$$\kappa = \lambda + \frac{2}{3}\mu, \tag{29}$$

and μ is the shear modulus. The second equality in Eq. (28) is a convenient formulation of the free energy in that the first term on the r.h.s. corresponds to pure uniform compression/dilation while the second term to pure shear.

Only two of the non-zero entries of tensor (26) are independent. It turns out that any isotropic tensor can be presented as the following spectral decomposition:[61]

$$\mathsf{L}[a\,,\,b] = a\mathsf{J} + b\mathsf{K}, \tag{30}$$

where a and b are some coefficients. The fourth-rank isotropic tensors J and K,

$$\begin{aligned}\mathsf{J}_{ijkl} &= \frac{1}{3}\delta_{ij}\delta_{kl},\\ \mathsf{K}_{ijkl} &= \frac{1}{2}\left(\delta_{ik}\delta_{jl} + \delta_{il}\delta_{jk} - \frac{2}{3}\delta_{ij}\delta_{kl}\right),\end{aligned}$$

are idempotent, i.e., they satisfy relations

$$\mathsf{JJ} = \mathsf{J} \qquad \text{and} \qquad \mathsf{KK} = \mathsf{K}, \tag{31}$$

and mutually "orthogonal",

$$\mathsf{JK} = \mathsf{KJ} = 0. \tag{32}$$

Acting on a symmetric second-rank tensor, say $\boldsymbol{\upsilon}$, the tensors J and K extract its hydrostatic (diagonal) and deviatoric (trace-less) parts respectively

$$\begin{aligned}\mathsf{J}_{ijkl}\upsilon_{kl} &= \frac{1}{3}\upsilon_{kk}\delta_{ij},\\ \mathsf{K}_{ijkl}\upsilon_{kl} &= \upsilon_{ij} - \frac{1}{3}\upsilon_{kk}\delta_{ij} \equiv {}'\upsilon_{ij}.\end{aligned} \tag{33}$$

In this notation, free energy (28) looks particularly simple:

$$e = \frac{\kappa}{2}\varepsilon_{ii}^2 + \mu\,{}'\varepsilon_{ij}{}^2. \tag{34}$$

Consequently, the elastic moduli tensor (26) can be written as

$$\mathsf{C} = \mathsf{L}[3\kappa\,,\,2\mu] = 2\mu\,\mathsf{L}\left[\frac{1+\nu}{1-2\nu}\,,\,1\right], \tag{35}$$

where ν is the Poisson ratio of the medium:

$$\nu \equiv \frac{1}{2\,(1+\mu/\lambda)} = \frac{3\kappa - 2\mu}{2(3\kappa+\mu)}. \tag{36}$$

Decomposition (30) simplifies the algebra for isotropic tensors considerably. For example, for two isotropic tensors $\mathsf{L}_1 = \mathsf{L}[a_1\,,\,b_1]$ and $\mathsf{L}_2 = \mathsf{L}[a_2\,,\,b_2]$, the sum and the product are given simply by

$$\mathsf{L}_1 + \mathsf{L}_2 = \mathsf{L}[a_1 + a_2\,,\,b_1 + b_2] \tag{37}$$

and

$$\mathsf{L}_1\mathsf{L}_2 = \mathsf{L}[a_1a_2\,,\,b_1b_2] \tag{38}$$

respectively. Also, the tensor equation $\mathsf{L}_1 = \mathsf{L}_2$ is equivalent to the system of two scalar equations, $a_1 = a_2$ and $b_1 = b_2$. The n-th power of the tensor can be computed using the formula

$$\mathsf{L}[a\,,\,b]^n = \mathsf{L}[a^n\,,\,b^n]\,, \tag{39}$$

where, note, n can be non-integer. Note that isotropic tensors commute with each other, a property which also holds for the cubic symmetry, but not so for other point symmetry groups.[61]

IV. RENORMALIZATION OF THE ELASTIC MODULI BY BUILT-IN STRESS: SETTING UP A CONTINUUM DESCRIPTION

Let us now consider a degenerate equilibrium aperiodic medium. The degeneracy is understood in the following way: The sample has a large number of alternative ground states, all of which are minima of the free energy. For each value of the free energy, there are an exponential number of alternative aperiodic minima. Such situation is realized in glassy liquids, where the number of alternative aperiodic states for a sample of volume V is given by $e^{\tilde{s}_c V/k_B}$, where $\tilde{s}_c$ is the configurational entropy of the liquid per unit volume. This entropy can be determined approximately by calorimetry, see Refs. 14 and 15 and references therein. The aperiodic free energy minima are metastable with respect to transitions between each other. These minima are also metastable with respect to the crystalline state, if any; throughout, we assume the nucleation barrier for crystallization is infinitely high.

Because the individual aperiodic minima are metastable, they are stable with respect to small, elastic deformation. The corresponding elastic moduli tensor is denoted with C_0. We will refer to these elastic constants as the "bare" constants. For simplicity, we assume they do not vary between minima, i.e., the minima are distinct but equivalent. In the language of replica-symmetry breaking, this equivalence corresponds to one-stage replica symmetry breaking.[62–64] Description at this low-stage replica-symmetry breaking is believed to be adequate in equilibrated liquids above the glass transition.[6,63,65–67]

Consider a macroscopic sample $\mathcal{B}$ of an equilibrated aperiodic solid, whose physical boundary is denoted with $\partial\mathcal{B}$. The internal—or "built-in"—stress, due to spatial interfaces between distinct aperiodic minima, is denoted with $\boldsymbol{\omega}(\mathbf{r})$, see Fig. 1. The RFOT theory has quantitatively characterized the activated reconfigurations between the distinct aperiodic minima, see review in Ref. 8. The presence of the built-in stress modifies the elastic response of the body analogously to how molecular dipoles modify the dielectric response of the liquid. Owing to the activated dynamics in the liquid, the built-in stress pattern is not steady, but relaxes on the time scale τ_α of the α-relaxation, even though the stress magnitude is steady on average. This is analogous to how polar molecules can rotate in a solution.

If an external traction force $\mathbf{t}(\mathbf{r})$ is applied to the boundary $\partial\mathcal{B}$ of $\mathcal{B}$, the resulting strain field $\mathbf{u}$ is a solution of the boundary value problem,

$$\begin{cases} \left(\sigma_{ij}+\omega_{ij}\right)_{,j}=0, \\ \sigma_{ij}n_j\Big|_{\partial\mathcal{B}}=t_i, \end{cases} \tag{40}$$

supplemented by the constitutive relation (Hooke's law):

$$\boldsymbol{\sigma}=\mathsf{C}_0\boldsymbol{\varepsilon}. \tag{41}$$

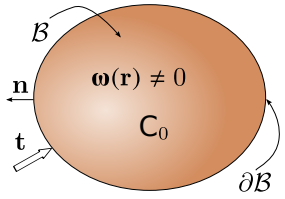

FIG. 1. Setup of Section IV: A homogeneous body $\mathcal{B}$ is subjected to external load in the form of a traction force $\mathbf{t}$ applied to the boundary $\partial\mathcal{B}$ of the body. The bare elastic constants of individual, aperiodic free energy minima are contained within the the fourth-rank tensor C_0. Unit vector $\mathbf{n}$ is an external normal to $\partial\mathcal{B}$. The built-in stress, denoted by the tensor field $\boldsymbol{\omega}(\mathbf{r})$, corresponds to the mismatch penalty at spatial interfaces between distinct free energy minima.

Equation (40) is Newton's 3rd law, the top and the bottom entry corresponding to the bulk and surface response respectively. The unit vector $\mathbf{n}$ is an external normal to $\partial\mathcal{B}$. The quantities $\boldsymbol{\sigma}$ and $\boldsymbol{\varepsilon}$ are, respectively, the elastic stress and strain inside $\mathcal{B}$. The strain $\boldsymbol{\varepsilon}$ is defined in Eq. (1).

Since individual minima respond purely elastically, the strain field ε_{ij} is *compatible*, $\operatorname{inc}\boldsymbol{\varepsilon}=0$, cf. Eq. (4). In contrast, the strain $\boldsymbol{\eta}(\mathbf{r})$ that corresponds to the internal stress $\boldsymbol{\omega}(\mathbf{r})$, $\boldsymbol{\omega}=\mathsf{C}_0\boldsymbol{\eta}$, can not be represented as a derivative of a single-valued deformation field. The field $\boldsymbol{\eta}$ is thus *incompatible*:

$$\left(\operatorname{inc}\boldsymbol{\eta}\right)_{ij}=-\epsilon_{ikl}\epsilon_{jmn}\eta_{ln,km}\neq 0. \tag{42}$$

Both $\mathbf{t}(\mathbf{r})$ and $\boldsymbol{\omega}$ cause deformation in $\mathcal{B}$, as already mentioned. Consequently, the elastic stress $\boldsymbol{\sigma}$ is a sum of two components:

$$\boldsymbol{\sigma}=\boldsymbol{\sigma}^{\mathrm{T}}+\boldsymbol{\sigma}^{\mathrm{S}}, \tag{43}$$

where the stress $\boldsymbol{\sigma}^{\mathrm{T}}$, produced by the surface traction, obeys

$$\begin{cases} \sigma^{\mathrm{T}}_{ij,j}=0, \\ \sigma^{\mathrm{T}}_{ij}n_j\Big|_{\partial\mathcal{B}}=t_i, \end{cases} \tag{44}$$

while the stress $\boldsymbol{\sigma}^{\mathrm{S}}$, produced by the source field $\boldsymbol{\omega}$, satisfies

$$\begin{cases} \left(\sigma^{\mathrm{S}}_{ij}+\omega_{ij}\right)_{,j}=0, \\ \sigma^{\mathrm{S}}_{ij}n_j\Big|_{\partial\mathcal{B}}=0. \end{cases} \tag{45}$$

The equation above follows from Eqs. (40) and (44). The elastic strain $\boldsymbol{\varepsilon}$ can be similarly written as a sum of two components,

$$\boldsymbol{\varepsilon}=\boldsymbol{\varepsilon}^{\mathrm{T}}+\boldsymbol{\varepsilon}^{\mathrm{S}}, \tag{46}$$

where the strain produced by the traction force $\mathbf{t}$ and the internal stress $\boldsymbol{\omega}$ are defined as

$$\boldsymbol{\sigma}^{\mathrm{T}}=\mathsf{C}_0\boldsymbol{\varepsilon}^{\mathrm{T}} \qquad \text{and} \qquad \boldsymbol{\sigma}^{\mathrm{S}}=\mathsf{C}_0\boldsymbol{\varepsilon}^{\mathrm{S}} \tag{47}$$

respectively. No built-in sources of stress lie at the boundary $\partial\mathcal{B}$ of the sample,

$$\boldsymbol{\omega}\Big|_{\partial\mathcal{B}} = 0, \tag{48}$$

and the present analysis is limited to symmetric sources

$$\omega_{ij} = \omega_{ji}. \tag{49}$$

The above boundary conditions for $\boldsymbol{\omega}$ are standard in treatments of defects in solids.[68] These conditions entail an important relation between the volume averages of $\boldsymbol{\sigma}^{\mathrm{S}}$ and $\boldsymbol{\omega}$,

$$\overline{\boldsymbol{\sigma}^{\mathrm{S}}} = \mathsf{C}_0\overline{\boldsymbol{\varepsilon}^{\mathrm{S}}} = -\overline{\boldsymbol{\omega}}, \tag{50}$$

which is straightforward to show by writing $\sigma^{\mathrm{S}}_{ij} = \sigma^{\mathrm{S}}_{ik}x_{k,j}$ and using Gauss's theorem together with Eq. (45).[69] Hereafter we use bars to indicate averaging over the volume V of $\mathcal{B}$. For instance,

$$\overline{\boldsymbol{\omega}} = \frac{1}{V}\int_{\mathcal{B}} \boldsymbol{\omega}\, \mathrm{d}V. \tag{51}$$

Since our liquid is equilibrated, ensemble averaging is equivalent to time averaging.

By Eq. (50), the built-in stress pattern $\overline{\boldsymbol{\omega}}$ automatically reflects the symmetry of C_0 in the limiting cases of a uniform liquid, $\mu_0 = 0$, and of an infinitely compressible body, $\kappa_0 = 0$. Indeed, $\mu_0 = 0 \Rightarrow \mathsf{C}_0 \propto \mathsf{J}$, and so Eq. (33) implies that for any $\overline{\boldsymbol{\varepsilon}^{\mathrm{S}}}$, the internal stress $\overline{\boldsymbol{\omega}}$ is purely hydrostatic. Likewise, in the other extreme $\kappa_0 = 0 \Rightarrow \mathsf{C}_0 \propto \mathsf{K}$, the tensor $\overline{\boldsymbol{\omega}}$ is purely deviatoric.

Next, we determine the linear response of body $\mathcal{B}$ to an external load. We define the effective elastic moduli C of $\mathcal{B}$ as a fourth-rank tensor connecting the volume average of the *total* stress in $\mathcal{B}$ with the volume average of the total elastic strain:

$$\int_{\mathcal{B}} (\boldsymbol{\sigma} + \boldsymbol{\omega})\, \mathrm{d}V = \int_{\mathcal{B}} (\mathsf{C}_0\boldsymbol{\varepsilon} + \boldsymbol{\omega})\, \mathrm{d}V \equiv \mathsf{C} \int_{\mathcal{B}} \boldsymbol{\varepsilon}\, \mathrm{d}V. \tag{52}$$

Note that by definition, C is spatially uniform and Eq. (52) is the elastic analog of Eq. (7). Definition (52) is equivalent to the relation

$$\int_{\mathcal{B}} \boldsymbol{\sigma}^{\mathrm{T}} \mathrm{d}V = \mathsf{C} \int_{\mathcal{B}} \boldsymbol{\varepsilon}\, \mathrm{d}V, \tag{53}$$

which is easy to show using Eqs. (43) and (50). The equation above relates quantities directly accessible in experiment: the average total load $\overline{\boldsymbol{\sigma}^{\mathrm{T}}}$ applied to $\mathcal{B}$ and the average resulted deformation $\overline{\boldsymbol{\varepsilon}}$ of $\mathcal{B}$. Using Eq. (46), we can further rewrite Eq. (53) as

$$\mathsf{C}_0\overline{\boldsymbol{\varepsilon}^{\mathrm{T}}} = \mathsf{C}(\overline{\boldsymbol{\varepsilon}^{\mathrm{T}}} + \overline{\boldsymbol{\varepsilon}^{\mathrm{S}}}). \tag{54}$$

In full correspondence with the above discussion of the symmetry of the built-in stress $\overline{\boldsymbol{\omega}}$, $\mathsf{C} \propto \mathsf{J}$ for a uniform liquid, $\mu_0 = 0$, while $\mathsf{C} \propto \mathsf{K}$ for an infinitely compressible solid, $\kappa_0 = 0$. We note that both cases correspond to *fixed* points on the $\nu_0 \mapsto \nu$ mapping, where ν_0 and ν are the bare and effective values of the Poisson ratio. Indeed, by Eq. (35), two isotropic fourth-rank tensors can be proportional to each other only if their Poisson ratios are equal. This notion will resurface in Section VII.

Since C should not depend on the configuration of the load and the shape of $\mathcal{B}$, we may conveniently assume a homogeneous $\boldsymbol{\varepsilon}^{\mathrm{T}}$. Under these circumstances, the 2nd equality in Eq. (52) yields:

$$\mathsf{C}\overline{\boldsymbol{\varepsilon}} = \mathsf{C}_0\overline{\boldsymbol{\varepsilon}} + \overline{\boldsymbol{\omega}}. \tag{55}$$

c.f. Eq. (7).

Thus, $\overline{\boldsymbol{\omega}}$ is a function of the average strain $\overline{\boldsymbol{\varepsilon}}$ in the material. Analogously to Eq. (8), one has in the linear-response regime:

$$\overline{\omega}_{ij} = \mathsf{X}^{\mathrm{S}}_{ijkl}\overline{\varepsilon}_{kl}, \tag{56}$$

where we define the static susceptibility $\mathsf{X}^{\mathrm{S}}_{ijkl}$ according to:

$$\mathsf{X}^{\mathrm{S}}_{ijkl} \equiv \left.\frac{\partial\overline{\omega}_{lm}}{\partial\overline{\varepsilon}_{kl}}\right|_{\overline{\boldsymbol{\varepsilon}}=0}, \tag{57}$$

c.f. Eq. (9). This results, together with Eq. (55), in a linear response-type relation between the effective and "bare" elastic moduli of $\mathcal{B}$:

$$\mathsf{C} = \mathsf{C}_0 + \mathsf{X}^{\mathrm{S}}. \tag{58}$$

Here we have used that $\overline{\boldsymbol{\omega}} = 0$ in the absence of external load. Equation (58) is the elastic analog of Eq. (10). It is valid for any symmetry of the tensor C_0. The following analysis is limited to isotropic elasticity, which is the simplest, yet most relevant case for amorphous materials. The "bare" elastic moduli, comprising the tensor C_0, will be labelled μ_0, κ_0, and ν_0; these are the shear and bulk modulus, and the Poisson ratio, respectively. We expect C to be isotropic as well, since, by definition, amorphous materials are isotropic in the long-wavelength limit. Therefore, the susceptibility X^{S} must be an isotropic tensor to satisfy Eq. (58). Consequently, the tensor equation (58) is equivalent to two scalar equations, as discussed Section III. The effective moduli comprising C will be labelled μ, κ, and ν. By Eq. (58) they can be determined with the knowledge of the response function (57).

V. INTERACTION BETWEEN SOURCES OF BUILT-IN STRESS

As in the dielectric case, calculation of the susceptibility (57) requires a specific microscopic model for the dynamics of $\boldsymbol{\omega}$. Here we explicitly obtain such a microscopic model, which is the elastic analog of the dipole-dipole interaction in electrostatics.

In an earlier publication,[29] which will be referred to as BL, we have put forth a minimal ansatz for the stress

distribution in equilibrated amorphous systems,[29] as explained in the Introduction, see Eq. (2). BL have shown that the dependence of the free energy F on the magnitude of built-in stress g is concave at small and large values of g, but has a convex portion at intermediate values of g. The low and high-g states can thus be interpreted as distinct phases separated by a nucleation barrier. The high g phase is aperiodic and vastly degenerate, the degeneracy originating from the multitude of mutual configurations of the degree of freedom $\boldsymbol{\eta}$, which has 5 independent components, in view of the constraint (3). Given sufficient steric stabilization for aperiodic structures, the high g phase can be made metastable implying the built-in stress can be *self-consistently* finite.

The interaction between the anharmonic degrees of freedom $\boldsymbol{\eta}$ is determined by integrating out the long-wavelength motions:[29]

$$\mathcal{H}_0 = \mathcal{H}_{\rm SE} + a^6 \sum_{m<n} \boldsymbol{\eta}(\mathbf{r}_n)\mathsf{C}_0\mathsf{G}(\mathbf{r}_m-\mathbf{r}_n)\mathsf{C}_0\boldsymbol{\eta}(\mathbf{r}_n), \quad (59)$$

where the double sums are over all bead pairs. The quantity $\mathcal{H}_{\rm SE}$ is the self-energy of the built-in stress in the absence of external load, see below. The coupling G is the Fourier transform,

$$\mathsf{G}(\mathbf{r}) = -\int_{|\mathbf{k}|\le\frac{\pi}{a}} \frac{d^3(\mathbf{k})}{(2\pi)^3}\cos(\mathbf{kr})\ \widetilde{\mathsf{G}}(\mathbf{k}), \quad (60)$$

of the following tensor:

$$\widetilde{G}_{ijml} = \frac{1}{\mu_0}\left(\delta_{im}\hat{k}_j\hat{k}_l + \delta_{il}\hat{k}_j\hat{k}_m + \delta_{jm}\hat{k}_i\hat{k}_l + \delta_{jl}\hat{k}_i\hat{k}_m - \frac{\lambda_0+\mu_0}{\lambda_0+2\mu_0}\hat{k}_i\hat{k}_j\hat{k}_m\hat{k}_l\right), \quad (61)$$

where $\hat{\mathbf{k}} \equiv \mathbf{k}/|\mathbf{k}|$. Recasting Eq. (59) in terms of the internal stress $\boldsymbol{\omega} = \mathsf{C}_0\boldsymbol{\eta}$ we obtain

$$\mathcal{H}_0 = \frac{1}{2}\int_{\mathcal{B}} \mathrm{d}V\, \boldsymbol{\omega}\mathsf{C}_0^{-1}\boldsymbol{\omega} + \frac{1}{2}\int_{\mathcal{B}}\mathrm{d}V\int_{\mathcal{B}}\mathrm{d}V'\omega_{ij}(\mathbf{r})\,\mathsf{G}_{ijlm}(\mathbf{r}-\mathbf{r}')\,\omega_{lm}(\mathbf{r}'), \quad (62)$$

where we assume the built-in stress $\boldsymbol{\omega}$ and deformation $\boldsymbol{\eta}$ are related by Hooke's law: $\boldsymbol{\omega} = \mathsf{C}_0\boldsymbol{\eta}$. Switching from discrete summation over bead sites to spatial integration is done according to the prescription $a^3\sum \to \int \mathrm{d}V$. The first integral on the r.h.s. of Eq. (62) corresponds to the self-energy from Eq. (59).

The expression for the coupling G between local sources of stress $\boldsymbol{\omega}$, Eq. (60), can be written out explicitly as:

$$\begin{aligned}\mathsf{G}_{ijml}(\mathbf{r}-\mathbf{r}') = &\frac{1}{64\pi^3\mu_0\,(1-\nu_0)}\left(\delta_{ip}\frac{\partial}{\partial x_j}+\delta_{jp}\frac{\partial}{\partial x_i}\right)\left(\delta_{ql}\frac{\partial}{\partial x_m}+\delta_{qm}\frac{\partial}{\partial x_l}\right)\\ &\times\left(2\,(1-\nu_0)\,\delta_{pq}\frac{\partial^2}{\partial x_s x_s}-\frac{\partial^2}{\partial x_p x_q}\right)\int_{|\mathbf{k}|\le\frac{\pi}{a}}\mathrm{d}\mathbf{k}\frac{e^{i\mathbf{k}(\mathbf{r}-\mathbf{r}')}}{k^4}.\end{aligned} \quad (63)$$

In the long-wavelength limit, $(r\to\infty)\Rightarrow(a\to 0)$, the above expression simplifies significantly as the integral reduces to $\int \mathrm{d}\mathbf{k}\exp[i\mathbf{kr}]/k^4 = -\pi^2 r$.[39] The stress-stress coupling, which we label in this approximation by $\mathsf{G}^{\rm A}$, can be now expressed via the well known Green tensor $\boldsymbol{\gamma}^{\rm A}$ for a point force inside an infinite, homogeneous, and isotropic medium (Kelvin's solution)[39] with the elastic moduli tensor C_0:

$$\mathsf{G}^{\rm A}_{ijml}(\mathbf{r}-\mathbf{r}') = \frac{1}{4}\left(\delta_{ip}\frac{\partial}{\partial x_j}+\delta_{jp}\frac{\partial}{\partial x_i}\right)\left(\delta_{ql}\frac{\partial}{\partial x_m}+\delta_{qm}\frac{\partial}{\partial x_l}\right)\gamma^{\rm A}_{pq}(\mathbf{r}-\mathbf{r}'), \quad (64)$$

where

$$\gamma^{\rm A}_{ij}(\mathbf{r}) = \frac{1}{16\pi\mu_0\,(1-\nu_0)}\frac{1}{r}\left[(3-4\nu_0)\,\delta_{ij}+\frac{x_i x_j}{r^2}\right]. \quad (65)$$

Note that, apart from the complicated tensorial form of the coupling, the (long-wavelength) distance dependence of $\mathsf{G}^{\rm A}$ is $\propto 1/r^3$, analogously to the electric dipole-dipole interaction. The tensor $\boldsymbol{\gamma}^{\rm A}(\mathbf{r})$ describes the response of the elastic medium to point-force localized at the origin. Note that this response diverges for a uniform liquid, $\mu_0 = 0$. This is expected since even an infinitesimal force causes an infinite displacement in a uniform liquid, and so linear elasticity is no longer applicable. Note that in the opposite extreme of an infinitely compressible body, $\kappa_0 = 0$ or $\nu_0 = -1$, the kernel $\boldsymbol{\gamma}^{\rm A}$ is well defined. As shown in Appendix A, $\mathsf{G}^{\rm A}(\mathbf{r})$ is the tensor describing the elastic response to a point-source of *stress* by an infinite, homogeneous, and isotropic medium. The elastic strain $\boldsymbol{\varepsilon}^{\rm S}$ produced by $\boldsymbol{\omega}$ can thus be written as

$$\boldsymbol{\varepsilon}^{\rm S}(\mathbf{r}) = \int_{\mathcal{B}}\mathrm{d}V'\mathsf{G}^{\rm A}(\mathbf{r}-\mathbf{r}')\boldsymbol{\omega}(\mathbf{r}'), \quad (66)$$

so that the Hamiltonian (62) becomes

$$\mathcal{H}_0 \approx \mathcal{H}_0^{\rm A} = \frac{1}{2}\int_{\mathcal{B}} {\rm d}V\, \boldsymbol{\omega}\left(\boldsymbol{\varepsilon}^{\rm S} + \mathsf{C}_0^{-1}\boldsymbol{\omega}\right), \qquad (67)$$

where the superscript "A" indicates that the long-wavelength limit of the Green's function is used.

In the presence of an external traction force, $\boldsymbol{\varepsilon}^{\rm T} \neq 0$, $\mathcal{H}_0$ must be supplemented by an appropriate coupling term. We will show systematically in Section VI, see Eq. (90), that this coupling is equal to the expected $\int_{\mathcal{B}} {\rm d}V\, \boldsymbol{\varepsilon}^{\rm T}\boldsymbol{\omega}$. Hence, the full Hamiltonian for the internal stress in the presence of the external load reads

$$\mathcal{H}^{\rm A} = \mathcal{H}_0^{\rm A} + \int_{\mathcal{B}} {\rm d}V\, \boldsymbol{\varepsilon}^{\rm T}\boldsymbol{\omega}. \qquad (68)$$

The linear response of the system to externally imposed deformation field $\boldsymbol{\varepsilon}^{\rm T}(\mathbf{r})$ is described, in the standard fashion, by the second order isothermal response function

$$\begin{aligned}\mathsf{X}_{ijkl}(\mathbf{r},\mathbf{r}') &= \left.\frac{\delta\langle\omega_{ij}(\mathbf{r})\rangle}{\delta\varepsilon^{\rm T}_{kl}(\mathbf{r}')}\right|_{\boldsymbol{\varepsilon}^{\rm T}=0} = \left.\frac{\delta}{\delta\varepsilon^{\rm T}_{kl}(\mathbf{r}')}\frac{\int\mathcal{D}\boldsymbol{\omega}\,\omega_{ij}(\mathbf{r})\exp\left[-\beta\mathcal{H}^{\rm A}\right]}{\int\mathcal{D}\boldsymbol{\omega}\exp\left[-\beta\mathcal{H}^{\rm A}\right]}\right|_{\boldsymbol{\varepsilon}^{\rm T}=0}\\ &= -\beta\Big[\langle\omega_{ij}(\mathbf{r})\omega_{kl}(\mathbf{r}')\rangle_0 - \langle\omega_{ij}(\mathbf{r})\rangle_0\langle\omega_{kl}(\mathbf{r}')\rangle_0\Big], \qquad (69)\end{aligned}$$

where the naught on the r.h.s. indicates averaging in zero field, $\boldsymbol{\varepsilon}^{\rm T} = 0$, by $\langle\cdots\rangle_0$. For instance,

$$\langle\boldsymbol{\omega}(\mathbf{r})\rangle_0 = \frac{\int\mathcal{D}\boldsymbol{\omega}\,\boldsymbol{\omega}(\mathbf{r})\,\exp[-\beta\mathcal{H}_0^{\rm A}]}{\int\mathcal{D}\boldsymbol{\omega}\,\exp[-\beta\mathcal{H}_0^{\rm A}]}. \qquad (70)$$

By the chain rule of differentiation,

$$\langle\omega_{ij}(\mathbf{r})\rangle = \int {\rm d}V' \left.\frac{\delta\langle\omega_{ij}(\mathbf{r})\rangle}{\delta\varepsilon^{\rm T}_{kl}(\mathbf{r}')}\right|_{\boldsymbol{\varepsilon}^{\rm T}=0} \varepsilon^{\rm T}_{kl}(\mathbf{r}'), \qquad (71)$$

and so the standard sum rule for the static isothermal susceptibility $\widetilde{\mathsf{X}}^{\rm S}$ holds:

$$\langle\omega_{ij}\rangle = \varepsilon^{\rm T}_{kl}\int {\rm d}V'\mathsf{X}_{ijkl}(\mathbf{r},\mathbf{r}') = \widetilde{\mathsf{X}}^{\rm S}_{ijkl}\varepsilon^{\rm T}_{kl}. \qquad (72)$$

We use the tilde to distinguish $\widetilde{\mathsf{X}}^{\rm S}$ from the susceptibility defined by Eq. (57) because it corresponds to the derivative of $\langle\boldsymbol{\omega}\rangle$ with respect to the average field $\overline{\boldsymbol{\varepsilon}}$, whereas $\widetilde{\mathsf{X}}^{\rm S}$ is equal to the derivative with respect to $\boldsymbol{\varepsilon}^{\rm T}$. The two fields are straightforwardly related by Eq. (54).

VI. CAVITY CONSTRUCTION FOR SUPERCOOLED LIQUIDS

Evaluation of the cumulant in Eq. (69) is prohibitively difficult to accomplish analytically for the model in Eq. (62). However, because of the Coulomb-like distance dependence of the interaction between point sources of force, we may proceed by analogy with the electric dipole-dipole interaction, for which Onsager's cavity method can be employed. The analogy between elasticity of stressed continua and electrostatics of polar dielectrics was noticed a long time ago and used primarily to study crystalline materials with a low concentration of defects.[60,70] Periodic lattices are anisotropic, which usually implies there at most few, discrete states of an individual defect.[71] The same thing can be said about orientational glasses, which are periodic crystals containing anisotropic substitutional impurities, whose orientations are random given sufficiently high density and/or low temperature.[72] Reorientational dynamics of such impurities lead to a marked temperature dependence of the elastic moduli.[72,73]

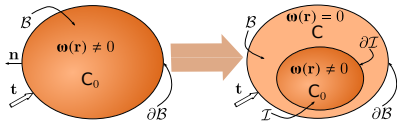

FIG. 2. Generalized cavity construction for the elasticity of supercooled liquids. The original amorphous body $\mathcal{B}$, characterized by the bare elastic moduli tensor C_0 and containing spatially-distributed built-in stress $\boldsymbol{\omega}$ is shown on the left. In the cavity construction, illustrated on the right, one treats explicitly a compact subset of the built-in sources of stress, while the response of the environment is approximated by that of an elastic continuum with effective constants C. The latter are found self-consistently for a given magnitude of the built-in stress.

We have shown earlier,[29] see also Sec. VII below, that constraint (3) is equivalent to fixing the length of a certain 6-component vector. Thus the structural dynamics of the built-in stress correspond to the rotations of interacting 6-vectors. This makes an effective field approximation for the elasticity of supercooled liquids conceptually very similar to that for the dielectric properties of polar liquids. In fact, as we will show below, it is possible to generalize Onsager's cavity construction to find a relation between the bare and renormalized elastic moduli of a supercooled liquid. This relation is controlled by the magnitude of the built-in stress, similarly to how the bare and renormalized dielectric constants are related via the magnitude of the molecular dipole in Eq. (18).

Consider an ellipsoidal region $\mathcal{I}$ inside the body $\mathcal{B}$. We will treat this region explicitly, whereby the region is characterized by bare elastic constants C_0 and an intrinsic distribution of built-in stress $\boldsymbol{\omega}$. In contrast, the built-

in stress *outside* the region will be treated effectively; we will approximate the response of the environment as an elastic continuum with effective elastic constants C, see Fig. 2. Our aim is to determine these effective elastic constants C self-consistently. We emphasize that this approach is not merely phenomenological, while being surely consonant with observation. Its validity has the same origin as the theory of dielectrics and stems from the fact that the electric field due to an infinite, uniformly charged plane is coordinate independent (within the individual half-spaces), leading to a uniform polarization-induced field inside a polarizable slab subject to a uniform external field. In turn, this notion stems from the $1/r$ dependence of the Green's function for electrostatic and elastic interactions, which has to do with the lack of mass for photons and phonons respectively.

Since both C_0 and C are assumed to be isotropic, all possible orientations of $\mathcal{I}$ in $\mathcal{B}$ are equivalent. The linear size of $\mathcal{B}$, $L_{\mathcal{B}}$, is assumed to be much larger than that of $\mathcal{I}$; consequently, we neglect the image forces produced by $\partial\mathcal{B}$ since the corresponding contribution is $\propto L_{\mathcal{B}}^{-3}$. A key feature of the construction is that it neglects correlations between the sources of built-in stress inside and outside of $\mathcal{I}$ for the purpose of estimating $\langle\boldsymbol{\omega}\rangle$. This is a good approximation, if the size of $\mathcal{I}$ is larger than the correlation length of the stress distribution $\boldsymbol{\omega}$. The thermodynamic average $\langle\boldsymbol{\omega}\rangle$ is then approximated by Boltzmann averaging over all structural states inside $\mathcal{I}$ only.

First off, the full elastic energy of $\mathcal{B}$ that contains an inclusion $\mathcal{I}$ containing sources of built-in stress $\boldsymbol{\omega}$ is equal to

$$\mathcal{E}_{el} = \frac{1}{2}\int_{\mathcal{B}} \mathrm{d}V\,(\boldsymbol{\sigma}+\boldsymbol{\omega})\left(\boldsymbol{\varepsilon}+\mathsf{C}_0^{-1}\boldsymbol{\omega}\right), \tag{73}$$

where the integrand is the product of the total (compatible and incompatible) stress, $\boldsymbol{\sigma}+\boldsymbol{\omega}$, and the total strain, $\boldsymbol{\varepsilon}+\mathsf{C}_0^{-1}\boldsymbol{\omega}$. The elastic stress $\boldsymbol{\sigma}$ and strain $\boldsymbol{\varepsilon}$ are solutions of Eq. (40), but since $\mathcal{B}$ now contains an inhomogeneity in the form of the elastic discontinuity at the region boundary $\partial\mathcal{I}$, Eq. (43) no longer holds. The total elastic stress now has to include a contribution from the stress "polarization" at the region boundary:

$$\boldsymbol{\sigma} = \boldsymbol{\sigma}^{\mathrm{T}} + \boldsymbol{\sigma}^{\mathrm{P}} + \boldsymbol{\sigma}^{\mathrm{S}}, \tag{74}$$

where

$$\boldsymbol{\sigma}^{\mathrm{T}} = \mathsf{C}\,\boldsymbol{\varepsilon}^{\mathrm{T}} \tag{75}$$

everywhere in $\mathcal{B}$; $\boldsymbol{\sigma}^{\mathrm{T}}$ satisfies (44). The quantity

$$\boldsymbol{\sigma}^{\mathrm{P}} = \begin{cases} \mathsf{C}\boldsymbol{\varepsilon}^{\mathrm{P}}, & \text{outside } \mathcal{I}, \\ \mathsf{C}_0\boldsymbol{\varepsilon}^{\mathrm{P}}, & \text{inside } \mathcal{I}, \end{cases} \tag{76}$$

is the stress produced by the boundary $\partial\mathcal{I}$, while $\boldsymbol{\sigma}^{\mathrm{S}}$ is the stress produced by $\boldsymbol{\omega}$. As before, $\boldsymbol{\sigma}^{\mathrm{S}}$ is given by the solution of (45) but the constitutive relations are now different between the region and the environment:

$$\boldsymbol{\sigma}^{\mathrm{S}} = \begin{cases} \mathsf{C}\boldsymbol{\varepsilon}^{\mathrm{S}}, & \text{outside } \mathcal{I}, \\ \mathsf{C}_0\boldsymbol{\varepsilon}^{\mathrm{S}}, & \text{inside } \mathcal{I}. \end{cases} \tag{77}$$

Analogously to $\boldsymbol{\sigma}^{\mathrm{S}}$, the stress $\boldsymbol{\sigma}^{\mathrm{P}}$ must satisfy the free traction boundary conditions on the surface of $\mathcal{B}$:

$$\sigma^{\mathrm{P}}_{ij} n_j\Big|_{\partial\mathcal{B}} = 0. \tag{78}$$

Next we use the cavity construction to evaluate the response function (57). First we need to establish a correspondence between the homogeneous set-up of Section IV and the present situation with an elastic discontinuity at the region boundary $\partial\mathcal{I}$. The traction forces in both cases are equal to each other analogously to how the dielectric displacement is not modified, on average, by introducing a cavity. Further, by Eqs. (75) and (53), we establish that the traction displacement $\boldsymbol{\varepsilon}^{\mathrm{T}}$ outside the inclusion $\mathcal{I}$ corresponds with the average strain $\overline{\boldsymbol{\varepsilon}}$ defined in Section IV. Thus, the static susceptibility X^{S} from Eq. (57) must be evaluated via

$$\mathsf{X}^{\mathrm{S}}_{ijkl} = \left.\frac{\partial\overline{\omega}_{ij}}{\partial\varepsilon^{\mathrm{T}}_{kl}}\right|_{\boldsymbol{\varepsilon}^{\mathrm{T}}=0}. \tag{79}$$

From here on, we assume $\boldsymbol{\sigma}^{\mathrm{T}}$ and $\boldsymbol{\varepsilon}^{\mathrm{T}}$ are homogeneous. Then, for an ellipsoidal region $\mathcal{I}$, $\boldsymbol{\varepsilon}^{\mathrm{P}}$ *inside* $\mathcal{I}$ is also homogeneous and is given by[61,69,74]

$$\boldsymbol{\varepsilon}^{\mathrm{P}} = \mathsf{S}\mathsf{Q}\left(\mathsf{C}-\mathsf{C}_0\right)\boldsymbol{\varepsilon}^{\mathrm{T}}, \tag{80}$$

where

$$\mathsf{Q} \equiv \left(\mathsf{C}-\left[\mathsf{C}-\mathsf{C}_0\right]\mathsf{S}\right)^{-1}, \tag{81}$$

and S is the so-called Eshelby tensor.[61] The Eshelby tensor appears in continuum mechanics as the solution to the following problem: Imagine that a region $\mathcal{I}$ inside a homogeneous elastic continuum with moduli C experiences a structural transformation, such as a martensitic transition. Under these circumstances the region would relax to attain a uniform stress-free strain $\boldsymbol{\varepsilon}^*$, *if* removed from the matrix. What is the deformation $\tilde{\boldsymbol{\varepsilon}}$ of the region $\mathcal{I}$, if it remains inside the matrix? Eshelby has shown that[75]

$$\tilde{\boldsymbol{\varepsilon}} = \mathsf{S}\,\boldsymbol{\varepsilon}^*, \tag{82}$$

where the tensor S is generally a function of the coordinate and depends on the shape of the region $\mathcal{I}$. If $\mathcal{I}$ is an ellipsoid, however, the Eshelby tensor is spatially uniform, and so is $\tilde{\boldsymbol{\varepsilon}}$. Despite its uniformity (for ellipsoidal $\mathcal{I}$), S is generally not isotropic, and so the order of multiplication in Eq. (80) matters. If, however, $\mathcal{I}$ *is* spherical, S does become isotropic:

$$\mathsf{S} = \frac{1}{3\,(1-\nu)}\,\mathsf{L}\left[1+\nu\,,\,\frac{2}{5}\,(4-5\nu)\right]. \tag{83}$$

The last equation applies also when the elastic moduli experience a discontinuity at the region boundary, the case we are interested here. Note that S depends only on the Poisson ratio of the matrix, i.e. the part of $\mathcal{B}$ outside

$\mathcal{I}$. Also, for $\nu = 1/5$, the Eshelby tensor is proportional to the unit tensor I,

$$\mathsf{S}\Big|_{\nu=1/5} = \frac{1}{2}\mathsf{I}, \tag{84}$$

so that $\tilde{\boldsymbol{\varepsilon}} = \boldsymbol{\varepsilon}^*/2$, i.e., $\tilde{\boldsymbol{\varepsilon}}$ and $\boldsymbol{\varepsilon}^*$ are related via a scalar. This is a peculiar situation, in which the self-consistent tensor equation (58) boils down to a single scalar equation, as we shall see in Sec. VII. Hereby the bulk and shear modulus are renormalized in equal measure so that ν remains equal to $\nu_0 = 1/5$.

In general, see Appendix B, the Eshelby tensor is related to the average of the Green tensor over the volume of the inclusion,

$$\mathsf{S} = -\int_{\mathcal{I}} \mathrm{d}V' \mathsf{G}^{\mathrm{A}}(\mathbf{r}-\mathbf{r}')\mathsf{C}, \tag{85}$$

where G^{A} is defined by Eq. (64) with μ_0 replaced by μ and ν_0 replaced by ν. Note, that since $\mathsf{G}^{\mathrm{A}} \propto \mu^{-1}$, while $\mathsf{C} \propto \mu$, see Eqs. (64), (65), and (35), the tensor S depends only on the Poisson ratio of the matrix for any shape of the region $\mathcal{I}$.

Below we will consider exclusively a spherical $\mathcal{I}$, in which case the tensor Q becomes

$$\mathsf{Q} = \frac{3(1-\nu)}{2\mu_0}\,\mathsf{L}\Big[\,\frac{1-2\nu_0}{(1+\nu)(1+\nu_0+2(\mu/\mu_0)\,[1-2\nu_0])}\,,\; \frac{5}{2\,[4-5\nu]+(\mu/\mu_0)\,[7-5\nu]}\,\Big]. \tag{86}$$

To determine the free energy $\mathcal{E}$ proper of the built-in stress pattern $\boldsymbol{\omega}$ in the presence of external load $\mathbf{t}$ we need to subtract from the full free energy $\mathcal{E}_{el}$ in Eq. (73) the elastic free energy of the body if it were homogeneous: $(1/2)\int_{\mathcal{B}} \boldsymbol{\sigma}^{\mathrm{T}}\boldsymbol{\varepsilon}^{\mathrm{T}}\mathrm{d}V$, and the work $\int_{\partial\mathcal{B}} \mathbf{t}\,(\mathbf{u}^{\mathrm{P}}+\mathbf{u}^{\mathrm{S}})\,\mathrm{d}S$ of the built-in stress and the stress due to the elastic discontinuity expended to distort the boundary of the macroscopic body $\mathcal{B}$:

$$\mathcal{E} = \mathcal{E}_{el} - \frac{1}{2}\int_{\mathcal{B}} \boldsymbol{\sigma}^{\mathrm{T}}\boldsymbol{\varepsilon}^{\mathrm{T}}\mathrm{d}V - \int_{\partial\mathcal{B}} \mathbf{t}\,(\mathbf{u}^{\mathrm{P}}+\mathbf{u}^{\mathrm{S}})\,\mathrm{d}S. \tag{87}$$

Multiple application of Gauss's theorem together with Eqs. (44)-(48), (78), and (80) allows one to recast $\mathcal{E}$ in terms of an integral over the inclusion only:

$$\mathcal{E} = \frac{1}{2}\int_{\mathcal{I}} \mathrm{d}V \Big(\boldsymbol{\omega}\boldsymbol{\varepsilon}^{\mathrm{S}} + \boldsymbol{\omega}\,\mathsf{C}_0^{-1}\boldsymbol{\omega} + \boldsymbol{\varepsilon}^{\mathrm{T}}\mathsf{C}\,(\mathsf{C}_0-\mathsf{C})\,\mathsf{Q}\boldsymbol{\varepsilon}^{\mathrm{T}} + \boldsymbol{\varepsilon}^{\mathrm{T}}\,(\mathsf{I}+\mathsf{C}\,\mathsf{Q})\,\boldsymbol{\omega} + \boldsymbol{\varepsilon}^{\mathrm{T}}\,(\mathsf{C}_0-\mathsf{C})\,\boldsymbol{\varepsilon}^{\mathrm{S}}\Big). \tag{88}$$

The derivation of this equation can be found in Chapter 4 of Mura's monograph;[69] here we only briefly review the result itself. The first two terms in the integrand have the same form as the earlier discussed Hamiltonian $\mathcal{H}_0^{\mathrm{A}}$, Eq. (67),

$$\mathcal{E}_0 = \frac{1}{2}\int_{\mathcal{I}} \mathrm{d}V \boldsymbol{\omega}\left(\boldsymbol{\varepsilon}^{\mathrm{S}} + \mathsf{C}_0^{-1}\boldsymbol{\omega}\right). \tag{89}$$

In important distinction from Eq. (67), the integration is over the inclusion $\mathcal{I}$ only. The third term, $(1/2)\boldsymbol{\varepsilon}^{\mathrm{T}}\mathsf{C}\,(\mathsf{C}_0-\mathsf{C})\,\mathsf{Q}\boldsymbol{\varepsilon}^{\mathrm{T}}$, is the potential energy due to the elastic inhomogeneity in the absence of built-in stress, i.e., when $\boldsymbol{\omega} = 0$; this term naturally vanishes for $\mathsf{C}_0 = \mathsf{C}$. Its sign is determined by the relative values of the bare and renormalized elastic constants $\mathsf{C}_0 - \mathsf{C}$. For instance, suppose that $\mu_0 < \mu$, $\kappa_0 < \kappa$, and there is no built-in stress other than the elastic discontinuity, i.e., $\boldsymbol{\omega} = 0$. Under these circumstances, the potential energy $\mathcal{E}$ is *negative* signifying that introduction of the inhomogeneity $\mathcal{I}$ makes the system (locally) unstable and may result, for instance, in cracking. Apropos, the third term in Eq. (88) provides the basis for the Griffith fracture criterion for a spherical inhomogeneity,[69] whereby the growth of the crack is limited by its surface energy. The last two terms in the integrand in Eq. (88) describe the interaction between the built-in stress $\boldsymbol{\omega}$ and the externally imposed strain $\boldsymbol{\varepsilon}^{\mathrm{T}}$.

Note that for a homogeneous $\mathcal{B}$, i.e. when $\mathsf{C} = \mathsf{C}_0$,

$$\mathcal{E}\Big|_{\mathsf{C}=\mathsf{C}_0} = \mathcal{E}_0 + \int_{\mathcal{I}} \mathrm{d}V\,\boldsymbol{\varepsilon}^{\mathrm{T}}\boldsymbol{\omega}, \tag{90}$$

since $\mathsf{I} + \mathsf{C}\mathsf{Q} = 2\mathsf{I}$ for $\mathsf{C} = \mathsf{C}_0$. This equation has the same form as Eq. (68), showing that $\mathcal{H}^{\mathrm{A}}$ is indeed the correct Hamiltonian for the stress distribution subject to an external field. Again, the integration in (90) is over the volume of the inclusion $\mathcal{I}$, not the whole body $\mathcal{B}$.

We finish this Section by writing down a formal expression for the susceptibility $\mathsf{X}(\mathbf{r},\mathbf{r}')$ for the generalized cavity construction shown on the right in Fig. 2. By Eqs. (79) and (88), we obtain:

$$\begin{aligned}\mathsf{X}_{ijkl}(\mathbf{r},\mathbf{r}') &= \frac{\delta}{\delta\varepsilon^{\mathrm{T}}_{kl}(\mathbf{r}')}\frac{\int \mathcal{D}\boldsymbol{\omega}\,\omega_{ij}(\mathbf{r})\exp\left[-\beta\mathcal{E}\right]}{\int \mathcal{D}\boldsymbol{\omega}\exp\left[-\beta\mathcal{E}\right]}\Bigg|_{\boldsymbol{\varepsilon}^{\mathrm{T}}=0} \\ &= -\beta\Big[\langle\omega_{ij}(\mathbf{r})\zeta_{kl}(\mathbf{r}')\rangle_0 - \langle\omega_{ij}(\mathbf{r})\rangle_0\langle\zeta_{kl}(\mathbf{r}')\rangle_0\Big],\end{aligned} \tag{91}$$

where

$$\boldsymbol{\zeta} = \frac{1}{2}\left[(\mathsf{I}+\mathsf{C}\mathsf{Q})\,\boldsymbol{\omega} - (\mathsf{C}-\mathsf{C}_0)\,\boldsymbol{\varepsilon}^{\mathrm{S}}\right], \tag{92}$$

and $\langle\cdots\rangle_0$, again, denotes thermodynamic averaging in zero external field, $\boldsymbol{\varepsilon}^{\mathrm{T}} = 0$.

The cavity construction is a reasonable approximation so long as the correlation length for the stress-stress interaction does not exceed the cavity size. It is possible to systematically improve on this approximation by including more sources of stress in the cavity $\mathcal{I}$ to explicitly account for many-particle effects. Such an approach can be implemented in simulations, as has been noted in the context of polar liquids.[76]

VII. SPECIFIC REALIZATION OF THE CAVITY CONSTRUCTION: THE CASE OF UNIFORM INTERNAL STRESS

One typically visualizes the Onsager cavity construction as an electric dipole in the center of an empty spherical cavity within a continuum dielectric. However, one might equally well think of the dipole moment due to the molecular dipole as uniformly *distributed* over the cavity. This will only modify the image field contribution to the energy of the molecular dipole. The image field is however aligned with the dipole itself and does not affect its orientation; Eq. (18) thus still applies. It will be convenient to pursue this "smeared source" approach in the elastic case as it readily produces closed form relationships between the bare and renormalized elastic constants. For a uniform $\boldsymbol{\omega}$ and a spherical inclusion $\mathcal{I}$,[61,69,75]

$$\boldsymbol{\varepsilon}^{\mathrm{S}} = -\mathsf{Q}\mathsf{S}\boldsymbol{\omega}, \tag{93}$$

and so the energy of the built-in stress inside the cavity, from Eq. (88), now reads:

$$\frac{\mathcal{E}}{v} = \frac{1}{2}\boldsymbol{\omega}\ \mathsf{G}\ \boldsymbol{\omega} + \boldsymbol{\varepsilon}^{\mathrm{T}}\ \mathsf{C}\ \mathsf{Q}\ \boldsymbol{\omega} + \frac{1}{2}\boldsymbol{\varepsilon}^{\mathrm{T}}\mathsf{C}\left(\mathsf{C}_0 - \mathsf{C}\right)\mathsf{Q}\ \boldsymbol{\varepsilon}^{\mathrm{T}}, \tag{94}$$

where v is the volume of $\mathcal{I}$, the tensor G is defined as

$$\mathsf{G} \equiv \mathsf{C}\left(\mathsf{I} - \mathsf{S}\right)\mathsf{Q}\ \mathsf{C}_0^{-1}, \tag{95}$$

and the Eshelby tensor S is given by (83). Equation (94) is Eq. (25.24) from Mura's monograph[69] written out explicitly for an isotropic solid. We note that the first and second quadratic forms on the r.h.s. of Eq. (94) are positive definite, while the third generally is not, as remarked earlier. Nevertheless, we shall see this term is always positive for the renormalized values of μ and κ that will be obtained self-consistently in the following.

The present, effective approach to the elasticity of aperiodic solids is, of course, an approximation. The choice of detailed implementation of the built-in stress is not unique and must be made depending on the circumstances.

In the first approach, we explicitly consider only a single source of built-in stress that is in direct contact with the effective elastic medium, analogously to the Onsager cavity construction. Hereby we fix the magnitude of $\mathcal{E}$ in the absence of external loading, $\boldsymbol{\varepsilon}^{\mathrm{T}} = 0$, while assuming the elastic constants are C_0 and C inside and outside the cavity, respectively:

$$\mathcal{E}^{\mathrm{G}} = \frac{v}{2}\boldsymbol{\omega}\mathsf{G}\boldsymbol{\omega} \equiv \frac{\theta^{\mathrm{G}}}{2\beta} = \mathrm{Const.} \tag{96}$$

Despite similarities between the dielectric and elastic cases, there is a fundamental distinction between how one can implement constraints on local sources of built-in stress in the two descriptions. In contrast with the dielectric case, the stress energy in Eq. (96) also includes the deformation energy of the *environment*. Indeed, while the dipole moment of a standalone molecule can be defined, the built-in stress within a small group of molecules only if it is inserted in an ill-fitting elastic matrix; the built-in stress thus cannot be defined on its own, i.e., without an environment.

In the second approach, we also fix the magnitude of the self-energy of the built-in stress in the absence of external load, but this time we use the *bare* elastic constants both inside and outside of the cavity. Substituting $\mathsf{C} = \mathsf{C}_0$ into the matrix G thus yields the following constraint:

$$\mathcal{E}^{\mathrm{F}} \equiv \frac{v}{2}\boldsymbol{\omega}\ \mathsf{C}_0^{-1}\left(\mathsf{I} - \mathsf{S}_0\right)\boldsymbol{\omega} \equiv \frac{\theta^{\mathrm{F}}}{2\beta} = \mathrm{Const.} \tag{97}$$

where S_0 is the Eshelby tensor for a medium with elastic moduli C_0. This way of constraining the built-in stress is appropriate when we wish to consider more than one sources explicitly. Clearly, each of these sources is inserted in the original medium characterized by the bare constants.

The third type of the constraint is equivalent to the constraint from Eq. (3) which corresponds to the original BL model.[29] Here one assumes that the self-interaction part of $\mathcal{E}^{\mathrm{F}}$ is fixed:

$$\mathcal{E}^{\mathrm{S}} \equiv \frac{v}{2}\boldsymbol{\omega}\mathsf{C}_0^{-1}\boldsymbol{\omega} = \frac{v}{2}\boldsymbol{\eta}\mathsf{C}_0\boldsymbol{\eta} \equiv \frac{\theta^{\mathrm{S}}}{2\beta} = \mathrm{Const}, \tag{98}$$

where $\boldsymbol{\eta} = \mathsf{C}_0^{-1}\boldsymbol{\omega}$, as discussed above, see Eq. (3).[29] According to the preceding discussion, this type of constraint does not explicitly consider the contribution of the medium to the full cost of the built-in stress. This may still be reasonable, if the inclusion size is large enough to sustain built-in stress on its own. Think of it as the smallest size of a standalone molecular cluster that has long-lived aperiodic minima, in addition to the lowest energy, crystalline minimum. Despite its limitations, the ansatz from Eq. (98) is of some formal value as it will allow us to recast the minimalistic BL model in an actual continuum fashion.

As already remarked in Section IV, we assume that all distinct aperiodic free energy minima are equivalent, implying that we can take the values of the constants in Eqs. (96)-(98) to be uniform in space. Below, we work out all three constraint types. The calculations are straightforward but tedious; they are mostly relegated to Appendix C. The technical gist of the calculation is as follows: We compute the partition function corresponding to the energy from Eq. (94), which requires integration with respect to the six components of the $\boldsymbol{\omega}$ tensor, subject to the constraints from Eqs. (96)-(98) for the three cases respectively. In practice, this is best done by switching to a special notation, in which rank-two tensors, such as $\boldsymbol{\omega}$ and $\boldsymbol{\varepsilon}^{\mathrm{T}}$, are represented as six-component vectors, while the rank-4 tensors, such as G, become 6-by-6 matrices; the latter happen to transform as tensors in this special notation.[77] The constraints (96)-(98) then

amount to fixing the magnitude of bilinear forms for the components of 6-vectors. This constraint can be further simplified by a coordinate transformation in the 6-space, upon which the quadratic form becomes the unit matrix. Consequently, each constraint is equivalent to fixing the length of a certain 6-vector, whose precise identity varies between the three cases.

A. Constraint 1: The "Onsager" limit

The self-energy energy $\mathcal{E}^{\rm G}$ from Eq. (96) reads explicitly, in terms of the components of the built-in stress $\boldsymbol{\omega}$, as

$$\frac{\mathcal{E}^{\rm G}}{v} = \frac{2\mu}{9\kappa_0}\,\frac{\omega_{ii}^2}{3\kappa_0+4\mu} + \frac{\mu}{4\mu_0}\,\frac{9\kappa+8\mu}{\mu\,(9\kappa+8\mu)+6\mu_0\,(\kappa+2\mu)}\,{}'\omega_{ij}^2, \tag{99}$$

where

$${}'\omega_{ij} \equiv \omega_{ij} - \frac{1}{3}\omega_{kk}\delta_{ij}, \tag{100}$$

is the deviatoric (trace-less) part of $\boldsymbol{\omega}$.

Clearly, in the limiting case of $\mu_0 = 0$ ($\nu_0 = 1/2$), only the hydrostatic component of $\boldsymbol{\omega}$ can be non-zero, consistent with the physical expectation that a uniform liquid cannot sustain built-in stress. Likewise, in the case of an infinitely compressible liquid, $\kappa_0/\mu_0 = 0$ ($\nu_0 = -1$), only the deviatoric part $\omega_{ij} = {}'\omega_{ij}$ is non-vanishing. In the spirit of the equipartition theorem, the two terms on the r.h.s. of Eq. (99) are expected to have comparable magnitudes. We thus tentatively conclude that as the Poisson ratio of the material changes from -1 to $1/2$—which corresponds to a decreasing shear modulus relative to the bulk modulus—the frozen-in stress pattern in the form of the built-in stress $\boldsymbol{\omega}$ switches character from mostly frozen-in shear to mostly frozen-in uniform compression/dilation, consistent with the BL analysis.[29]

We show in Appendix C that Eq. (58), which connects the effective and bare elastic moduli, now becomes:

$$\mathsf{C} = \mathsf{C}_0\left(\mathsf{I} - \frac{\theta^{\rm G}}{6}\left[\mathsf{I}-\mathsf{S}\right]^{-1}\right), \tag{101}$$

where the Eshelby matrix for the effective medium is given in Eq. (83); it depends on the effective Poisson ratio ν. The above equation thus can be used to determine the effective moduli self-consistently.

According to Sec. III, the tensor equation (101) is equivalent to the system of two scalar equations, viz.,

$$\begin{cases} \dfrac{\mu}{\mu_0} &= 1+\theta^{\rm G}\left(\dfrac{1}{7-5\nu}-\dfrac{1}{2}\right); \\ \dfrac{\mu}{\mu_0} &= \dfrac{(1+\nu_0)\,(4-\theta^{\rm G}\,[1-\nu]-8\nu)}{4\,(1-2\nu_0)\,(1+\nu)}, \end{cases} \tag{102}$$

where the dimensionless magnitude $\theta^{\rm G}$ of the built-in stress energy is defined in Eq. (96).

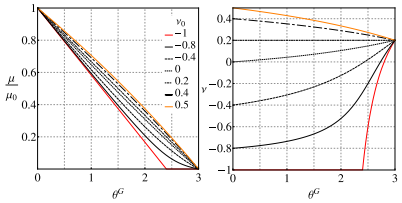

FIG. 3. Constraint (96): **(a)** Renormalization μ/μ_0 of the shear modulus as a function of the dimensionless energy $\theta^{\rm G} = 2\beta\mathcal{E}^{\rm G}$ of the built-in stress, for the constraint in Eq. (96). **(b)** The effective Poisson ratio ν as a function of $\theta^{\rm G}$ for several values of of the bare Poisson ratio ν_0. In both panels, the orange lines correspond to the uniform-liquid limit for the bare medium, $\nu_0 \to 1/2$, while the red lines correspond to an infinitely compressible solid, $\nu_0 \to -1$. The legends are identical in the two panels.

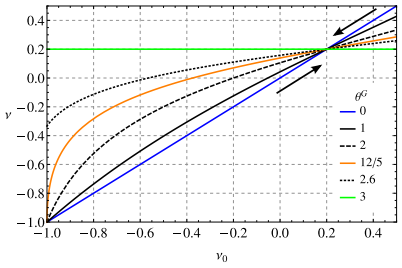

FIG. 4. Constraint (96): Dependence of the effective Poisson ratio ν on its bare value ν_0 for several values of the built-in stress $\theta^{\rm G}$. The three fixed points at $\nu = -1, 1/5, 1/2$ are discussed in text. The arrows indicate the direction of the flow on $\nu_0 \mapsto \nu$ mapping.

The system of equations (102) can be readily solved, the solution graphically summarized on Figs. 3-5. This is the main result of the present work, besides the formal developments in Sections III-VI that lay foundation of continuum mechanics for structurally degenerate solids.

It is immediately clear from Eq. (102) that the effective shear modulus is always reduced from its bare value in the presence of built-in stress, since $-1 \le \nu_0, \nu \le 1/2$. This down-renormalization comes about because the built-in stress enhances the local elastic field, according to Eq. (23) and in contrast with the dielectric case.

Because of the physical constraint $\mu \ge 0$—which guarantees mechanical stability with respect to shear, by Eq. (28)—the dimensionless built-in stress $\theta^{\rm G}$ has a limiting value: $\theta^{\rm G} \le 3$. Beyond this limiting value of built-in stress, the aperiodic solid becomes a uniform liquid. The dependences of the μ/μ_0 ratio and the Poisson ratio on $\theta^{\rm G}$ are shown in Fig. 3(a) and (b) respectively. When the compressibility diverges, $\nu_0 \to -1$, the μ/μ_0 ratio approaches the line $1 - 5\theta^{\rm G}/12$, while in the limit of uniform liquid $\nu_0 \to 1/2$, the ratio tends to the line $6\,(3-\theta^{\rm G})\,/\,(18-\theta^{\rm G})$.

We have already discussed that the $\nu_0 \mapsto \nu$ mapping has two trivial fixed points corresponding to the uniform

liquid ($\nu = \nu_0 = 1/2$) and infinitely compressible solid ($\nu = \nu_0 = -1$). At the uniform liquid fixed point, the bulk modulus vanishes at any value of the built-in stress:

$$\frac{\kappa}{\kappa_0} \xrightarrow[\nu_0 \to 1/2]{} 16\left(\frac{1}{2} - \nu_0\right)\frac{(6-\theta^{\rm G})(3-\theta^{\rm G})}{\theta^{\rm G}(18-\theta^{\rm G})}. \qquad (103)$$

At the same time, the μ/κ ratio remains finite in this limit, except when $\theta^{\rm G} \to 0$:

$$\lim_{\nu_0 \to 1/2} \frac{\mu}{\kappa} = \frac{3\theta^{\rm G}}{4(6-\theta^{\rm G})}, \qquad (104)$$

or, equivalently,

$$\lim_{\nu_0 \to 1/2} \nu = 1 + \frac{4}{\theta^{\rm G} - 8}. \qquad (105)$$

Because the renormalized μ/κ ratio remains finite even as the bare ratio vanishes—see Fig. 4—the uniform-liquid fixed point is *discontinuous*, except when there is no built-in stress to begin with, $\theta^{\rm G} = 0$.

The present formalism is internally-consistent in that it yields an infinitely-compressible and, hence, marginally stable system, if one supposes that a uniform liquid could sustain built-in stress of finite magnitude, see Eq. (103). In other words, we have established that the internal stress is self-consistently zero in the uniform-liquid regime. On the other hand, because only non-zero values of the built-in stress are meaningful in the aperiodic-crystal state, the discontinuity at $\nu_0 = 1/2$ (for finite $\theta^{\rm G}$) in Eq. (105) means that the RFOT transition from the uniform liquid to the equilibrium aperiodic solid is discontinuous, while the built-in stress also emerges at the transition in a discontinuous fashion. In the RFOT theory, the discontinuity is signalled by a discrete jump of the force constant for the effective Einstein oscillator from zero to a number of order $100/a^2$.[4,78–81]

The $\nu_0 = -1$ fixed point is continuous for sufficiently low values of the built-in stress but becomes discontinuous when $\theta^{\rm G} > 12/5$, where the discontinuity in the Poisson ratio is equal to:

$$\lim_{\nu_0 \to -1} \nu = 1 - \frac{4}{5(\theta - 2)}, \qquad (106)$$

In this regime, μ and κ vanish simultaneously while their ratio remains finite, similarly to Eq. (104):

$$\lim_{\nu_0 \to -1} \frac{\kappa}{\mu} = -\frac{4(5\theta^{\rm G} - 12)}{3(5\theta^{\rm G} - 18)}, \qquad \text{for} \qquad \theta^{\rm G} > \frac{12}{5}. \qquad (107)$$

The physical meaning of the $\nu = -1$ fixed is not entirely clear at present. It may correspond to the mechanical stability limit of a non-degenerate vibrational ground state. We anticipate that such a stability limit could be realized in nature during pressure-induced amorphization,[82–85] which is possible when the crystalline structure is relatively open. The latter situation may be also realized in high spatial dimensions, where the highest possible filling fraction may be achieved in *aperiodic* packings.[86]

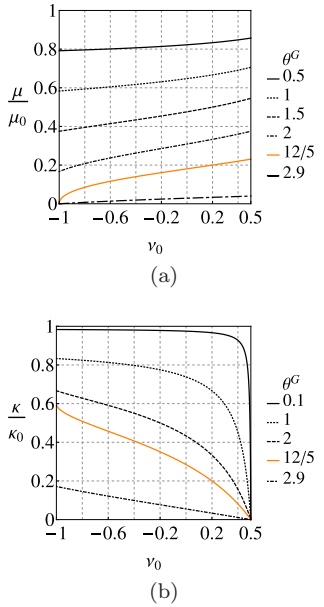

FIG. 5. Constraint (96): Dependences of the ratios μ/μ_0 and κ/κ_0 on the bare value of the Poisson ratio ν_0 for several values of $\theta^{\rm G}$, in panels **(a)** and **(b)** respectively. The orange line corresponds to $\theta^{\rm G} = 12/5$, which separates the two regimes in which the fixed point $\nu = -1$ is continuous and discontinuous respectively. Note that the derivative of μ/μ_0 as a function of ν_0 diverges at $\theta^{\rm G} = 12/5$, $\nu_0 \to -1$, whereby $\mu/\mu_0 \propto \sqrt{(1+\nu_0)}/2\sqrt{5}$. The κ/κ_0 ratio is zero at $\nu = 1/2$ for a finite $\theta^{\rm G}$, however small. This ratio is finite when $\theta^{\rm G}$ is strictly zero.

In addition, according to Figs. 3(b) and 4, there is a non-trivial fixed point at $\nu_0 = \nu = \nu_0^{\rm FP} = 1/5$, independent of $\theta^{\rm G}$. This fixed point formally stems from the property of the Eshelby tensor, by which $\mathsf{S} \propto \mathsf{I}$ for $\nu = 1/5$, according to Eq. (84). Relation (101) then dictates that $\mathsf{C} \propto \mathsf{C}_0$, which is possible only if $\nu_0 = \nu$. The proportionality of the Eshelby tensor to the unit matrix means that at this special value of the Poisson ratio, the relative weight of shear and uniform deformation of a relaxed standalone inclusion does not change after it is inserted in the matrix. At this fixed point, the self-consistency relation (101) boils down to a simple:

$$\mu^{\rm FP} = \mu_0\left(1 - \frac{\theta^{\rm G}}{3}\right). \qquad (108)$$

The non-trivial fixed point is *attractive*, because $\nu > \nu_0$ for $\nu_0 < \nu_0^{\rm FP}$, and $\nu < \nu_0$ for $\nu_0 > \nu_0^{\rm FP}$. Note also that ν approaches $\nu_0^{\rm FP}$ as $\theta^{\rm G}$ tends to its limiting value 3, for all values of ν_0. Conversely, the *trivial* fixed points are unstable, as indicated by the arrows in Fig. 4.

The behavior of the effective moduli, in relation to their bare counterparts, is shown in Fig. 5. Here we ex-

plicitly see that like the shear modulus, the bulk modulus is also always down-renormalized. Finally, the renormalization flow in the (μ, κ) plane is shown in Fig. 8 in Appendix D.

B. Constraint 2: Built-in stress inserted in bare medium

When written out explicitly, the constraint in Eq. (97) reads as follows:

$$\frac{\mathcal{E}^{\mathrm{F}}}{v} = \frac{1}{3\kappa_0 + 4\mu_0}\left(\frac{2\mu_0}{9\kappa_0}\omega_{ii}^2 + \frac{9\kappa_0 + 8\mu_0}{20\mu_0}\,{}'\omega_{ij}^2\right). \quad (109)$$

Note the *adiabatic* values of the elastic moduli satisfy the relation $3\kappa_s + 4\mu_s = 3\rho c_l^2$, where ρ is the mass density of the body and c_l is the speed of longitudinal phonons.[30] The expressions we have written for the elastic free energy density are equilibrium, implying the elastic moduli are isothermal. The isothermal and adiabatic shear moduli are equal to each other[30], while the adiabatic bulk modulus exceeds its isothermal value, although usually not by much.

Similarly to the preceding case, we observe that the identity of the built-in stress interpolates between the frozen-in shear and uniform deformation as the Poisson ratio is varied from -1 to $1/2$. The relation between the bare and effective elastic moduli now contains modified Bessel functions and is significantly more complicated than in the preceding case, see Eq. (C28) in Appendix C. We present the numerical solution of this equation in Fig. 6.

According to Fig. 6(a), the dependence of μ/μ_0 on θ^{F} is affected by the value of ν_0 only weakly. The magnitude of the renormalization itself remains significant, however there is no longer a limiting value to the built-in stress. This seems consonant with the lower degree of self-consistency in the current set-up, whereby the outside of the cavity is no longer represented by the effective medium.

The $\theta^{\mathrm{F}} = \mathrm{Const}$ case exhibits the same three fixed points as the preceding constraint, including their assignment in terms of being attractive or repulsive, Fig. 6(b). In contrast, only the uniform-liquid point is now discontinuous, the size of the discontinuity vanishing in the absence of built-in stress. The dependence of the jump of the Poisson ratio on the magnitude of built-in stress is presented in the inset of Fig. 6(b). If we invoke the notion from the Introduction Section that the built-in stress must be finite in magnitude, we again arrive at a result that the uniform liquid turns into an aperiodic solid in a discontinuous fashion. Still, this result is not as strong as in the Onsager limit, in which the finite jump in the built-in stress itself, at the transition, was established self-consistently. Finally, it can be shown analytically that the non-trivial fixed point is located, again, at $\nu_0^{\mathrm{FP}} = 1/5$, see Appendix C.

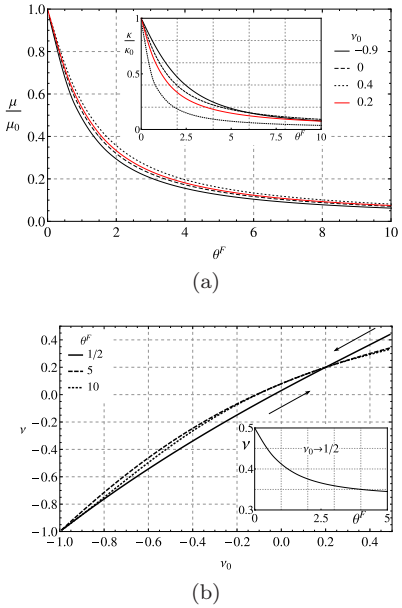

(a)

(b)

FIG. 6. Constraint (97): graphical summary of the solution of Eq. (C28). **(a)** Renormalization μ/μ_0 of the shear modulus as a function of the dimensionless stress energy $\theta^{\mathrm{F}} = 2\beta\mathcal{E}^{\mathrm{F}}$ from Eq. (97) for several values of the bare Poisson ratio ν_0. The black lines are numerical solutions of Eq. (C28). The red line gives the analytical solution at the fixed point $\nu = \nu_0 = 1/5$, Eq. (C34). **(b)** Dependence of the effective Poisson ratio ν on its bare value ν_0 for several values of θ^{F}. The arrows indicate the direction of the flow on the $\nu_0 \mapsto \nu$ mapping. The inset shows the dependence of ν on θ^{F} for $\nu_0 \to 1/2$.

C. Constraint 3: BL model

The relation between the bare and renormalized moduli, which is given as Eq. (C36) in Appendix C, also must be solved numerically, see Fig. 7.

In contrast with the two preceding cases, the trivial fixed points are now continuous in the full parameter range. Interestingly, the relevance of the fixed points—in the RG sense of the word—is now reversed. The fixed point at $\nu_0 = 1/5$ is now repulsive, while the trivial fixed points at $\nu_0 = -1$ and $\nu_0 = 1/2$ are stable, see Fig. 7(b).

The repulsive nature of the $\nu_0^{\mathrm{FP}} = 1/5$ point is consonant with the BL finding that at the value of the Poisson ratio $1/5$, the mean-field limit of the Hamiltonian (59) has a continuous transition from an Ising-like ferromagnet to a Heisenberg-like ferromagnet with 5-spins. The two regimes, when well-developed, correspond to frozen-in uniform and frozen-in shear stress patterns respectively. Exactly at the transition, the two types of frozen-in stress patterns are marginally stable with respect to each other. We thus conclude that the $\nu_0^{\mathrm{FP}} = 1/5$ fixed point is analogous to an isospin-like degeneracy between shear and uniform deformation.

Note the uniform-liquid now transitions to the aperiodic solid *continuously*. This unphysical feature stems from the limitation of the BL ansatz (98) discussed ear-

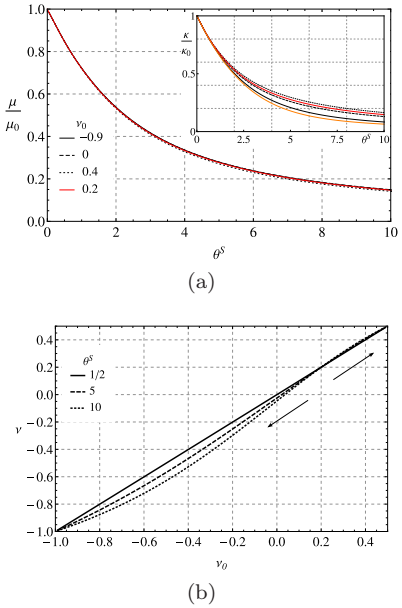

FIG. 7. Constraint (98): graphical summary of the solution of Eq. (C37). **(a)** Renormalization μ/μ_0 of the shear modulus as a function of the dimensionless stress energy $\theta^{\rm s} = 2\beta\mathcal{E}^{\rm s}$ from Eq. (98) for several values of the bare Poisson ratio ν_0. The black lines are numerical solutions of Eq. (C28). The red line gives the analytical solution at the fixed point $\nu = \nu_0 = 1/5$. The orange line in the inset gives the analytical solution in the $\mu_0 \to 0$ limit, Eq. (C39). **(b)** Dependence of the effective Poisson ratio ν on its bare value ν_0 for several values of $\theta^{\rm s}$. The arrows indicate the direction of the flow on the $\nu_0 \mapsto \nu$ mapping. In contrast with the preceding cases, this fixed point is now unstable.

lier.

VIII. CONCLUSION

We have developed a continuum mechanics description of the elasticity exhibited by equilibrium, degenerate aperiodic solids. Such aperiodic solids are exemplified by liquids that flow by local activated transitions between distinct aperiodic free energy minima. The transition to activated transport from the ordinary, collisional transport typical of uniform liquids may occur above or below the fusion temperature, depending on the fragility of the liquid.[1] In ordinary liquids—as opposed to colloids, for instance—the structural glass transition is always preceded by the emergence of activated transport.[2]

Despite allowing the liquid to flow, albeit on very long timescales, the activated transitions are rare events relative to molecular vibrations.[1,2] Yet already a mesoscopic region relaxes at a rate high enough to prevent one from defining a vibrational ground state unambiguously in this region. At the same time, the vibrational response of such a degenerate solid is well described phenomenologically using the standard elasticity theory, apart from the presence of a large dissipative component.

The present work shows why such an elastic description is possible despite the lack of a unique vibrational ground state. Such uniqueness is, of course, very basic to the theory of elasticity, similarly to how the uniqueness of vacuum is basic to electrodynamics. To tackle the problem of the vast structural degeneracy of equilibrium aperiodic solids, we have employed the microscopic picture advanced by the RFOT theory, which constructively demonstrates that such aperiodic crystals represent a mosaic of distinct solutions of the free energy functional.[6,7] The physical boundaries between distinct solutions of the free energy functional are strained regions that cannot be removed by elastic deformation, but only by a discontinuous transition to the corresponding periodic crystal, if the latter exists. The strained regions thus correspond to *built-in* stress. The extent and concentration of such strained regions is dictated by thermodynamics; near the glass transition, the corresponding lengthscale is 2-4 nm in actual materials.[7,9]

The specific implementation of the built-in stress employed in this work originates from our earlier approach,[29] in which the molecular motions at short and long wavelengths are treated on a separate footing. The short-wavelength modes give rise to a frozen-in stress pattern, while the long-wavelength modes corresond to elastic excitations of the material for a given configuration of the frozen-in short-lengthscale motions. Despite its tensorial nature, the interaction between such local sources of strain bears similarities to the electric dipole-dipole interaction. This deep analogy between continuum electrostatics and mechanics allows one to formulate the problem of interaction between sources of built-in stress similarly to how Onsager[17] and others[18–20] have derived the theory of dielectric response starting from a microscopic model of a polar liquid as an equilibrium assembly of molecular dipoles. In complete analogy with the dielectrics, the mechanical response is determined by the elastic properties of individual free energy minima (which corresponds to the response of vacuum in electrodynamics), the magnitude of the built-in stress (which corresponds to the molecular dipole moment), and temperature. In the language of Yoshino and Mezard,[32,33] the elastic properties of individual minima and the macroscopic liquid correspond to inter- and intra-basin elastic moduli. In an important distinction, here we consider response at *finite*, even if low, frequencies.

Yet in contrast with the dielectric case—whereby polarized dipoles screen the external field—the elastic response is *enhanced* by the sources of built-in stress. As a result, there is a liming value to the built-in stress that can be supported by aperiodic crystal. In actual substances, the magnitude of the built-in stress is determined by the molecular interaction. Here, we have treated the magnitude of built-in stress as a flexible parameter. We have found three fixed points in the mapping between the bare and renormalized elastic constants, the renormalization stemming from the presence and relaxation of the built-in stress. Two of the fixed points correspond

to the uniform liquid, in which the shear modulus is identically zero, and to an infinitely compressible solid. We find that the transition from the uniform liquid to the equilibrium aperiodic crystal is discontinuous, in agreement with earlier conclusions of the RFOT theory.[4,78–81]

There is also a somewhat surprising fixed point at which the Poisson ratio stays constant after the renormalization. The corresponding value $\nu = 1/5$ is special in that it signals a degeneracy of sorts between the shear and uniform deformation. If a spherical inclusion is inserted in an elastic continuum, and both are characterized by this particular value of the Poisson ratio, the relative weights of the shear and uniform deformation inside and outside will be equal to each other. Note that the equality of the Poisson ratios between two different materials in contact implies that a single acoustic wave will refract into a single wave. In the absence of such equality, the refraction will result in two waves because the transverse and longitudinal sound will refract differently. The $\nu = 1/5$ fixed point turns out to coincide with the critical point in the mean-field limit of the BL model,[29] in which the aperiodic solid makes a transition between two types of frozen-in stress patterns corresponding to shear and uniform deformation respectively.

As pointed out in the Introduction, the present work specifically addresses the effects of structural *degeneracy* on the vibrational response of an equilibrium aperiodic solid, as opposed to effects of aperiodicity in a fully *stable* lattice. A stable aperiodic lattice exhibits non-affine displacements and spatially-heterogeneous elasticity, leading to Rayleigh scattering of acoustic waves. These fascinating features of harmonic (!) aperiodic lattices have been proposed as the cause of the apparent excess of vibrational states in glasses often referred to as the Boson Peak, requiring however that the lattice be near its mechanical stability limit.[28,53,87] In the absence of such marginal stability, purely elastic scattering seems too weak to account for the apparent magnitude of phonon scattering at Boson Peak frequencies.[88,89] In contrast, the presence of structural degeneracy leads to an entirely distinct, *resonant* type of phonon scattering. The resonances are due to local transitions between distinct free energy minima of the aperiodic solid.[9,41] A RFOT-based analysis shows these elastic resonances do account quantitatively for the apparent magnitude of the heat capacity and phonon scattering both in the temperature range corresponding to the Boson Peak[41,90] and, at the same time, at lower, sub-Kelvin temperatures where the so called two-level systems[91] dominate the thermal properties of the glass.[9,41]

It is hoped that despite some computational complexity, the present description will help advance applications of the RFOT theory to actual materials. The present description enables one to realize the BL program of modeling activated transport in liquids via a spin model on a fixed lattice, while not requiring the full knowledge of the complicated, many-body interactions between actual molecules. Instead, only the elastic constants and the bead size are needed as the microscopic input. In this regard, it would be interesting to investigate a case in which the bare elasticity is not isotropic.

ACKNOWLEDGMENTS

The authors thank Peter G. Wolynes for insight and valuable discussions. This work has been supported by the National Science Foundation (CHE-0956127), the Alfred P. Sloan Research Fellowship, and the Welch Foundation Grant E-1765.

Appendix A: The Green tensor for a point stress source

Consider an infinite medium with a distribution of body force $\mathbf{f}(\mathbf{r})$, which is non-zero over a finite domain. The distribution produces an elastic response described by the deformation field $\mathbf{u}$ satisfying the following boundary value problem,

$$\begin{cases} \sigma_{ij,j} + f_i = 0, \\ \mathbf{u}(\mathbf{r}) \xrightarrow[r\to\infty]{} 0, \end{cases} \tag{A1}$$

where the stress $\boldsymbol{\sigma}$ is related to the deformation $\mathbf{u}$ by the constitutive relation $\boldsymbol{\sigma} = \mathsf{C}_0\boldsymbol{\varepsilon}$ and the elastic strain $\boldsymbol{\varepsilon}$ is defined in Eq. (1). One can solve Eq. (A1) by Fourier transforming $\mathbf{u}$,[39] the result given by

$$u_i(\mathbf{r}) = \int \mathrm{d}V' \gamma^{\mathrm{A}}_{ij}(\mathbf{r}-\mathbf{r}') f_i(\mathbf{r}'), \tag{A2}$$

where the second-rank Green tensor $\boldsymbol{\gamma}^{\mathrm{A}}$ for isotropic elasticity is provided in Eq. (65).

The force balance for the built-in stress is $\sigma_{ij,j}+\omega_{ij,j} = 0$. Substituting this equation, together with Eq. (A1), into Eq. (A2) and integrating by parts yields:[92]

$$u_i(\mathbf{r}) = -\frac{1}{2}\int \mathrm{d}V' \left[\gamma^{\mathrm{A}}_{ij,l'} + \gamma^{\mathrm{A}}_{il,j'}\right] \omega_{jl}(\mathbf{r}'). \tag{A3}$$

Differentiating the above equation w.r.t. x_j and symmetrizing, according to the definition of $\boldsymbol{\varepsilon}$ from Eq. (1), we obtain that the strain field resulting from built-in stress $\boldsymbol{\omega}$ can be calculated using a Green's function which is essentially the second derivative of the kernel γ^{A}_{ij}:

$$\varepsilon_{ij} = \int \mathrm{d}V' \mathsf{G}^{\mathrm{A}}_{ijml}(\mathbf{r},\mathbf{r}')\omega_{ml}(\mathbf{r}'), \tag{A4}$$

where

$$\begin{aligned} \mathsf{G}^{\mathrm{A}}{}_{ijml}(\mathbf{r},\mathbf{r}') = -\frac{1}{4}\left(\delta_{ip}\frac{\partial}{\partial x_j} + \delta_{jp}\frac{\partial}{\partial x_i}\right) \\ \times \left(\delta_{ql}\frac{\partial}{\partial x'_m} + \delta_{qm}\frac{\partial}{\partial x'_l}\right)\gamma^{\mathrm{A}}_{pq}(\mathbf{r},\mathbf{r}'), \end{aligned} \tag{A5}$$

Noting that $\frac{\partial}{\partial x'_i} = -\frac{\partial}{\partial x_i}$, when acting on a function of $\mathbf{r}-\mathbf{r}'$, one obtains Eq. (64).

Appendix B: The physical meaning of the Eshelby tensor

The Eshelby tensor S comes about in continuum mechanics as the solution to the following problem.[75] Consider an infinite isotropic body $\mathcal{B}$ characterized by an elastic moduli tensor C. Suppose a local region, call it $\mathcal{I}$, undergoes a martensitic or some other structural transformation, thus resulting in a stress distribution $\boldsymbol{\omega}$ due to the mismatch between the transformed region and the matrix. This stress is incompatible; it is a source of a body force which causes a compensating elastic strain $\boldsymbol{\varepsilon}^{\mathrm{S}}$ to appear in the surrounding elastic medium. As we just saw in Appendix A, $\boldsymbol{\varepsilon}^{\mathrm{S}}$ can be calculated using Eq. (A4), where the integration is now over $\mathcal{I}$ only, since $\boldsymbol{\omega}$ is zero outside. Further, if $\boldsymbol{\omega}$ is uniform, it can be moved outside the integral, and so $\boldsymbol{\varepsilon}^{\mathrm{S}}$ is now related to the volume average of G^{A} over $\mathcal{I}$:

$$\varepsilon^{\mathrm{S}}_{ij}(\mathbf{r}) = \omega_{ml}\int_{\mathcal{I}} \mathrm{d}V' G^{\mathrm{A}}_{ijml}(\mathbf{r}-\mathbf{r}'). \tag{B1}$$

J. D. Eshelby showed that for an elliptical $\mathcal{I}$, the volume average of G^{A} in (B1) does not depend on $\mathbf{r}$, if $\mathbf{r}\in\mathcal{I}$. Thus, $\boldsymbol{\varepsilon}^{\mathrm{S}}$ is homogeneous inside $\mathcal{I}$.[75] The Eshelby solution is usually written in terms of the "eigenstrain" $\boldsymbol{\varepsilon}^{*}$ related to $\boldsymbol{\omega}$ by

$$\boldsymbol{\varepsilon}^{*} = -\mathsf{C}^{-1}\boldsymbol{\omega}. \tag{B2}$$

The tensor relating the eigenstrain $\boldsymbol{\varepsilon}^{*}$ with the actual elastic strain $\boldsymbol{\varepsilon}^{\mathrm{S}}$ *inside* $\mathcal{I}$ is called the Eshelby tensor S:

$$\boldsymbol{\varepsilon}^{\mathrm{S}} = \mathsf{S}\,\boldsymbol{\varepsilon}^{*}. \tag{B3}$$

Eq. (B1) and (B2) imply

$$\boldsymbol{\varepsilon}^{\mathrm{S}} = -\left[\int_{\mathcal{I}} \mathrm{d}V' \mathsf{G}^{\mathrm{A}}(\mathbf{r}-\mathbf{r}')\right]\mathsf{C}\,\boldsymbol{\varepsilon}^{*},$$

which by Eq. (B3) yields Eq. (85).

Appendix C: Calculation of the partition function and local susceptibility for uniformly distributed built-in stress

It is possible to formulate the linear elasticity so that rank-2 tensors are presented as six component vectors, $\varepsilon_{ij}\to\varepsilon_{\alpha}$, $\alpha=1,2,3,4,5,6$. Specifically: $\varepsilon_1=\varepsilon_{11}$, $\varepsilon_2=\varepsilon_{22}$, $\varepsilon_3=\varepsilon_{33}$, $\varepsilon_4=\sqrt{2}\varepsilon_{23}$, $\varepsilon_5=\sqrt{2}\varepsilon_{31}$, $\varepsilon_5=\sqrt{2}\varepsilon_{12}$.[77] To avoid confusion, the components of the 6-vectors will be labeled with Greek indexes. The original rank-4 tensors now become rank-2 tensors, as in $\mathsf{C}_{ijkl}\to\mathsf{C}_{\alpha\gamma}$. Any isotropic tensor can be diagonalized according to:

$$\Big(\mathsf{L}[a\,,\,b]\Big)_{\alpha\beta} = \mathsf{U}_{\alpha\gamma}\Big(\mathsf{D}[a\,,\,b]\Big)_{\gamma\delta}\big(\mathsf{U}^{\top}\big)_{\delta\beta}, \tag{C1}$$

where

$$\mathsf{U} = \begin{pmatrix} 1/\sqrt{3} & -1/\sqrt{6} & -1/\sqrt{2} & 0 & 0 & 0\\ 1/\sqrt{3} & -1/\sqrt{6} & 1/\sqrt{2} & 0 & 0 & 0\\ 1/\sqrt{3} & \sqrt{2}/\sqrt{3} & 0 & 0 & 0 & 0\\ 0 & 0 & 0 & 1 & 0 & 0\\ 0 & 0 & 0 & 0 & 1 & 0\\ 0 & 0 & 0 & 0 & 0 & 1 \end{pmatrix} \tag{C2}$$

is the tensor constructed from the eigenvectors of $\mathsf{L}[a\,,\,b]$, and the symbol $\mathsf{D}[a\,,\,b]$ labels a diagonal tensor of the form

$$\mathsf{D}[a\,,\,b] = \begin{pmatrix} a & 0 & 0 & 0 & 0 & 0\\ 0 & b & 0 & 0 & 0 & 0\\ 0 & 0 & b & 0 & 0 & 0\\ 0 & 0 & 0 & b & 0 & 0\\ 0 & 0 & 0 & 0 & b & 0\\ 0 & 0 & 0 & 0 & 0 & b \end{pmatrix}. \tag{C3}$$

Note that U does not depend on a and b, $\mathsf{U}\mathsf{U}^{\top}=\mathsf{I}$, and the determinant $|\mathsf{U}|=-1$.

1. Constraint 1, Eq. (96)

We begin with the first constraint, Eq. (96). Define a 6-vector $\boldsymbol{\psi}$ such that

$$\boldsymbol{\omega} \equiv \sqrt{\frac{2\mathcal{E}^{\mathrm{G}}}{v}}\mathsf{G}^{-1/2}\boldsymbol{\psi}. \tag{C4}$$

Substituting Eq. (C4) into constraint (96) we get in the 6-vector representation:

$$\psi_{ij}\psi_{ij} = \psi_{\alpha}\psi_{\alpha} = |\boldsymbol{\psi}|^2 = 1. \tag{C5}$$

Thus, the constraint (96) is equivalent to fixing the length of the 6-vector $\boldsymbol{\psi}$. All structural states of a homogeneous $\boldsymbol{\omega}$ in the spherical cavity $\mathcal{I}$ allowed by (96) are now mapped onto all possible orientations of the unit 6-vector $\boldsymbol{\psi}$ analogously to how the configurations of a polar molecule in a dielectric solution are mapped onto all possible orientations of its dipole moment. The thermodynamic average $\langle\boldsymbol{\omega}\rangle$ can be computed via the thermodynamic average of $\langle\boldsymbol{\psi}\rangle$, cf. Eq. (15),

$$\langle\boldsymbol{\psi}\rangle = \frac{\int \mathrm{d}\Omega_6 \boldsymbol{\psi} e^{-\beta\mathcal{E}}}{\int \mathrm{d}\Omega_6 e^{-\beta\mathcal{E}}}, \tag{C6}$$

where the integration is carried out over the solid angle in the six dimensional spherical coordinate system,

$$\begin{aligned}\mathrm{d}\Omega_6 = &\sin^4 x_1 \sin^3 x_2 \sin^2 x_3 \sin x_4\\ &\times \mathrm{d}x_1\mathrm{d}x_2\mathrm{d}x_3\mathrm{d}x_4\mathrm{d}x_5,\end{aligned} \tag{C7}$$

$x_{\alpha}\in[0,\pi]$, for $\alpha<5$, and $x_5\in[0,2\pi]$.

The potential energy $\mathcal{E}$ can be written in terms of $\boldsymbol{\psi}$ in a form completely analogous to the dielectric case, Eq. (14):

$$\mathcal{E} = \mathcal{E}^{\mathrm{G}} + \boldsymbol{\zeta}\boldsymbol{\psi} + \frac{v}{2}\boldsymbol{\varepsilon}^{\mathrm{T}}\mathsf{C}\,[\mathsf{C}_0-\mathsf{C}]\,\mathsf{Q}\boldsymbol{\varepsilon}^{\mathrm{T}}, \tag{C8}$$

where

$$\boldsymbol{\zeta} \equiv \sqrt{2v\mathcal{E}^{\mathrm{G}}}\mathsf{CQG}^{-1/2}\boldsymbol{\varepsilon}^{\mathrm{T}}. \tag{C9}$$

Clearly, $\mathcal{E}$ depends on the cosine of the angle between $\boldsymbol{\zeta}$ and $\boldsymbol{\psi}$ only. Thus, analogously to the dielectric case, the partition function can be calculated exactly:

$$\begin{aligned} Z &= \int \mathrm{d}\Omega_6 e^{-\beta\mathcal{E}} = \\ &= \frac{8\pi^2}{3} e^{-\beta\mathcal{E}^{\mathrm{G}}} e^{-\frac{v}{2}\beta\boldsymbol{\varepsilon}^{\mathrm{T}}\mathsf{C}[\mathsf{C}_0-\mathsf{C}]\mathsf{Q}\boldsymbol{\varepsilon}^{\mathrm{T}}} \int_0^{\pi} \mathrm{d}x_1 \sin^4 x_1 e^{-y\cos x_1} \\ &= 8\pi^3 \frac{I_2(y)}{y^2} e^{-\beta\mathcal{E}^{\mathrm{G}}} e^{-\frac{v}{2}\beta\boldsymbol{\varepsilon}^{\mathrm{T}}\mathsf{C}[\mathsf{C}_0-\mathsf{C}]\mathsf{Q}\boldsymbol{\varepsilon}^{\mathrm{T}}}, \end{aligned} \tag{C10}$$

where $y \equiv \beta|\boldsymbol{\zeta}|$ and we have used the integral representation of the modified Bessel function $I_n(y)$ from Eq. (9.6.18) of Ref. 93. Such integrals often appear in the context of the $O(n)$ model.[94]

To compute the expectation value of the internal stress we first note that by Eq. (94):

$$\begin{aligned} \frac{\partial F}{\partial \varepsilon^{\mathrm{T}}_\alpha} &= -\frac{1}{\beta}\frac{1}{Z}\frac{\partial Z}{\partial \varepsilon^{\mathrm{T}}_\alpha} \\ &= \left(v\mathsf{C}\mathsf{Q}\langle\boldsymbol{\omega}\rangle\right)_\alpha + \left(v\mathsf{C}\left[\mathsf{C}_0-\mathsf{C}\right]\mathsf{Q}\boldsymbol{\varepsilon}^{\mathrm{T}}\right)_\alpha. \end{aligned} \tag{C11}$$

One the other hand, differentiation of Eq. (C10) yields

$$\frac{\partial F}{\partial \varepsilon^{\mathrm{T}}_\alpha} = v\left(\mathsf{C}\left[\mathsf{C}_0-\mathsf{C}\right]\mathsf{Q}\boldsymbol{\varepsilon}^{\mathrm{T}}\right)_\alpha - \frac{1}{\beta}\frac{I_3(y)}{I_2(y)}\frac{\partial y}{\partial \varepsilon^{\mathrm{T}}_\alpha}, \tag{C12}$$

where

$$\frac{\partial y}{\partial \varepsilon^{\mathrm{T}}_\alpha} = 2\beta^2 v\frac{\mathcal{E}^{\mathrm{G}}}{y}\left(\mathsf{C}^2\mathsf{Q}^2\mathsf{G}^{-1}\boldsymbol{\varepsilon}^{\mathrm{T}}\right)_\alpha. \tag{C13}$$

Here we have used Eq. (9.6.28) of Ref. 93. Combining Eqs. (C11) and (C12) yields

$$\begin{aligned} \langle\omega_\alpha\rangle &= -\frac{1}{\beta v}\left(\mathsf{CQ}\right)^{-1}_{\alpha\gamma}\frac{I_3(y)}{I_2(y)}\frac{\partial y}{\partial \varepsilon^{\mathrm{T}}_\gamma} \\ &= -2\beta\mathcal{E}^{\mathrm{G}}\frac{I_3(y)}{yI_2(y)}\left(\mathsf{CQG}^{-1}\boldsymbol{\varepsilon}^{\mathrm{T}}\right)_\alpha. \end{aligned} \tag{C14}$$

Note that $\lim_{y\to 0} I_3(y)/(yI_2(y)) = \frac{1}{6}$. Upon differentiation of Eq. (C4), we obtain for the static susceptibility

$$\mathsf{X}^{\mathrm{S}}_{\alpha\gamma} = -\frac{\beta\mathcal{E}^{\mathrm{G}}}{3}\left(\mathsf{CQG}^{-1}\right)_{\alpha\gamma}, \tag{C15}$$

Combining this with Eqs. (96), (95), and (58) yields Eq. (101).

2. Constraint 2, Eq. (97)

Now we define the vector $\boldsymbol{\psi}$ according to:

$$\boldsymbol{\omega} = \sqrt{\frac{2\mathcal{E}^{\mathrm{F}}}{v}}\mathsf{R}\,\mathsf{U}\,\boldsymbol{\psi}, \tag{C16}$$

where

$$\begin{aligned} \mathsf{R} &\equiv \sqrt{\mathsf{C}_0\left(\mathsf{I}-\mathsf{S}_0\right)^{-1}} = \sqrt{(3\kappa_0+4\mu_0)} \\ &\times \mathsf{L}\left[\sqrt{\frac{3\kappa_0}{4\mu_0}}, \sqrt{\frac{10\mu_0}{9\kappa_0+8\mu_0}}\right] \end{aligned} \tag{C17}$$

and the square root of the tensor is computed using Eq. (39).

With these definitions, the potential energy $\mathcal{E}$ from Eq. (94) can be written as:

$$\begin{aligned} \frac{\mathcal{E}}{v} &= \frac{\mathcal{E}^{\mathrm{F}}}{v}\boldsymbol{\psi}\,\mathsf{D}\,\boldsymbol{\psi} + \sqrt{\frac{2\mathcal{E}^{\mathrm{F}}}{v}}\boldsymbol{\varepsilon}^{\mathrm{T}}\mathsf{C}\,\mathsf{Q}\,\mathsf{R}\,\mathsf{U}\boldsymbol{\psi} \\ &- \frac{1}{2}\boldsymbol{\varepsilon}^{\mathrm{T}}\mathsf{C}\left[\mathsf{C}-\mathsf{C}_0\right]\mathsf{Q}\,\boldsymbol{\varepsilon}^{\mathrm{T}}, \end{aligned} \tag{C18}$$

where $\mathsf{D} = \mathsf{U}^{\top}\mathsf{RGRU} = \mathsf{D}[\gamma_1, \gamma_2]$ is a diagonal matrix, see (C3), with

$$\begin{aligned} \gamma_1 &= \frac{3(\mu/\mu_0)(1-\nu_0)}{1+2(\mu/\mu_0)(1-2\nu_0)+\nu_0}, \\ \gamma_2 &= \frac{15(\mu/\mu_0)(1-\nu_0)(7-5\nu)}{(7-5\nu_0)\left(8+7(\mu/\mu_0)-5\nu\left[2+(\mu/\mu_0)\right]\right)}. \end{aligned} \tag{C19}$$

Eqs. (79) and (C16) yield:

$$\mathsf{X}^{\mathrm{S}}_{\alpha\gamma} = \sqrt{\frac{2\mathcal{E}^{\mathrm{F}}}{v}}\left(\mathsf{RU}\right)_{\alpha\zeta}\left.\frac{\partial\langle\psi_\zeta\rangle}{\partial\varepsilon^{\mathrm{T}}_\gamma}\right|_{\boldsymbol{\varepsilon}^{\mathrm{T}}=0}, \tag{C20}$$

where the derivative on the r.h.s. can be rewritten, using Eqs. (C6) and (C18), as

$$\begin{aligned} \left.\frac{\partial\langle\psi_\alpha\rangle}{\partial\varepsilon^{\mathrm{T}}_\gamma}\right|_{\boldsymbol{\varepsilon}^{\mathrm{T}}=0} &= -\beta\sqrt{\frac{2\mathcal{E}^{\mathrm{F}}}{v}}\left[\langle\psi_\alpha\psi_\zeta\rangle - \langle\psi_\alpha\rangle\langle\psi_\zeta\rangle\right]_{\boldsymbol{\varepsilon}^{\mathrm{T}}=0} \\ &\times\left(\mathsf{U}^{\top}\mathsf{R}\,\mathsf{Q}\,\mathsf{C}\right)_{\zeta\gamma}. \end{aligned} \tag{C21}$$

The angular integration in Eq. (C6) can be performed analytically since for $\boldsymbol{\varepsilon}^{\mathrm{T}} = 0$,

$$\begin{aligned} \left.\frac{\mathcal{E}}{\mathcal{E}^{\mathrm{F}}}\right|_{\boldsymbol{\varepsilon}^{\mathrm{T}}=0} &= \boldsymbol{\psi}\mathsf{D}\boldsymbol{\psi} \\ &= \frac{1}{2}\left[\gamma_1+\gamma_2+(\gamma_1-\gamma_2)\cos 2x_1\right], \end{aligned} \tag{C22}$$

where x_1 is from Eq. (C7). By symmetry, $\langle\psi_\alpha\rangle_{\boldsymbol{\varepsilon}^{\mathrm{T}}=0} = 0$. A straightforward calculation yields

$$\left.\langle\psi_\alpha\psi_\zeta\rangle\right|_{\boldsymbol{\varepsilon}^{\mathrm{T}}=0} = \Big(\mathsf{D}[1-5s(p)\,,\,s(p)]\Big)_{\alpha\zeta}, \tag{C23}$$

where

$$p \equiv \frac{1}{4}\theta^{\mathrm{F}}\left(\gamma_1-\gamma_2\right). \tag{C24}$$

and

$$s\left(p\right)=\frac{\int_0^\pi dx_1\sin^6 x_1 e^{-p\cos 2x_1}}{\int_0^\pi dx_1\sin^4 x_1 e^{-p\cos 2x_1}} \\ =\frac{p\left(4p-1\right)I_0(p)+\left(2+p\left[4p-3\right]\right)I_1(p)}{10p\left[2pI_0(p)+\left[2p-1\right]I_1(p)\right]}. \tag{C25}$$

Substitution of these results into Eq. (C20) gives:

$$\mathsf{X}^{\rm S}=-\theta^{\rm F}\,\mathsf{C}_0\mathsf{C}\left(\mathsf{I}-\mathsf{S}_0\right)^{-1}\mathsf{Q}\mathsf{L}[1-5s(p)\,,\,s(p)]\,, \tag{C26}$$

where $\theta^{\rm F}=2\beta\mathcal{E}^{\rm F}$, Eq. (97). Subsequently,

$$\left(\mathsf{I}-\mathsf{S}_0\right)\left(\mathsf{C}+\left[\mathsf{C}_0-\mathsf{C}\right]\mathsf{S}\right)\left(\mathsf{C}_0-\mathsf{C}\right) \\ =\theta^{\rm F}\,\mathsf{C}_0\mathsf{C}\,\mathsf{L}[1-5s(p)\,,\,s(p)]\,. \tag{C27}$$

Dividing out both sides of the last equation by C_0^2 yields the sought relation between the bare and renormalized elastic moduli:

$$\left(\mathsf{I}-\mathsf{S}_0\right)\left(\mathsf{Y}+\left[\mathsf{I}-\mathsf{Y}\right]\mathsf{S}\right)\left(\mathsf{I}-\mathsf{Y}\right) \\ =\theta^{\rm F}\,\mathsf{Y}\,\mathsf{L}[1-5s(p)\,,\,s(p)]\,, \tag{C28}$$

where

$$\mathsf{Y}\equiv\mathsf{C}\mathsf{C}_0^{-1}=(\mu/\mu_0)\mathsf{L}\left[\frac{1+\nu}{1-2\nu}\frac{1-2\nu_0}{1+\nu_0}\,,\,1\right]. \tag{C29}$$

As discussed in Sec. III, the tensorial Eq. (C28) is equivalent to a system of two scalar equations. Analytical solution of Eq. (C28) is possible in the high temperature limit, where $\mathsf{L}[1-5s(p)\,,\,s(p)]=\mathsf{I}/6$. However, the resulting expression is too bulky to give here.

The non-trivial fixed point can be found analytically usign the high temperature limit. Taylor-expanding $s(p)$ from Eq. (C25): $s(p)=\frac{1}{6}+\frac{p}{72}+O\left(p^2\right)$, yields, together with Eq. (C28):

$$6\left(\mathsf{I}-\mathsf{S}_0\right)\left(\mathsf{Y}+\left[\mathsf{I}-\mathsf{Y}\right]\mathsf{S}\right)\left(\mathsf{I}-\mathsf{Y}\right)=\theta^{\rm F}\,\mathsf{Y}. \tag{C30}$$

To test for the presence of the fixed point we substitute $\nu=\nu_0$. Then, $\mathsf{Y}=(\mu/\mu_0)\mathsf{I}$, $\mathsf{S}=\mathsf{S}_0$, and the equation simplifies to read

$$6\left(\mathsf{I}-\mathsf{S}_0\right)\left((\mu/\mu_0)+\left[1-(\mu/\mu_0)\right]\mathsf{S}_0\right)\left(1-(\mu/\mu_0)\right) \\ =\theta^{\rm F}(\mu/\mu_0)\mathsf{I}. \tag{C31}$$

Since the r.h.s. of Eq. (C31) is proportional to I, the solution is possible only if S_0 is proportional to I as well, and so, by Eq. (83) with $\nu=\nu_0$:

$$\nu_0=\nu_0^{\rm FP}=\frac{1}{5}, \tag{C32}$$

Remarkably, at the fixed point $(\gamma_1-\gamma_2)_{\nu=\nu_0=\nu_0^{\rm FP}}=0$, so that

$$\mathsf{L}[1-5s(p)\,,\,s(p)]\,\Big|_{\nu=\nu_0=\nu_0^{\rm FP}}=\frac{1}{6}\mathsf{I}, \tag{C33}$$

see Eq. (C28). This means that at the fixed point, Eqs. (C31) and (C32)—which were obtained by Taylor-expanding with respect to p from Eq. (C24)—are valid for all values of $\theta^{\rm F}$. Then, selecting the positive root of Eq. (C31) at the fixed point, we obtain,

$$\mu^{\rm FP}=\left(\sqrt{1+\left[\frac{\theta^{\rm F}}{3}\right]^2}-\frac{\theta^{\rm F}}{3}\right)\,\mu_0. \tag{C34}$$

Since the the (μ/μ_0) ratio depends on ν_0 only weakly, see Fig. 6, Eq. (C34) represents a good approximate expression for the temperature dependence of the effective shear modulus for materials with ν_0 numerically close to 0.2.

3. Constraint 3, Eq. (98)

The preceding calculation is easily adopted for the constraint (98) by substituting for the matrix R, Eq. (C17), the following matrix:

$$\widetilde{\mathsf{R}}=\mathsf{C}_0^{1/2}, \tag{C35}$$

so we can switch to the constraint (98) by simply removing the factor $\mathsf{I}-\mathsf{S}_0$ from the formulas. This yields the following relation between the bare and renormalized moduli:

$$\left(\mathsf{C}-\left[\mathsf{C}-\mathsf{C}_0\right]\mathsf{S}\right)\left(\mathsf{C}-\mathsf{C}_0\right) \\ =-\theta^{\rm S}\,\mathsf{C}_0\mathsf{C}\,\mathsf{L}[1-5s(\tilde{p})\,,\,s(\tilde{p})] \tag{C36}$$

or

$$\left(\mathsf{Y}+\left[\mathsf{I}-\mathsf{Y}\right]\mathsf{S}\right)\left(\mathsf{I}-\mathsf{Y}\right)=\theta^{\rm S}\,\mathsf{Y}\,\mathsf{L}[1-5s(\tilde{p})\,,\,s(\tilde{p})]\,, \tag{C37}$$

where

$$\tilde{p}=(3/4)(\mu/\mu_0)\theta^{\rm S}\left(3-5\nu+\nu_0\left[15\nu-13\right]\right) \\ \times\quad\left(1+\nu_0+2(\mu/\mu_0)\left[1-2\nu_0\right]\right)^{-1} \\ \times\quad\left(8+7(\mu/\mu_0)-5\nu\left[(\mu/\mu_0)+2\right]\right)^{-1}. \tag{C38}$$

Similarly to Eq. (C28), one can solve Eq. (C37) in the high temperature limit, but the resulting expression is very complicated; we only show it graphically in Fig. 7. Note that unlike Eq. (C27), Eq. (C36) possesses three *continuous* fixed points. Indeed, if $\nu_0=1/2$ then $\mathsf{C}_0\propto\mathsf{J}$, see Eq. (35). Consequently, the r.h.s. of Eq. (C36) is proportional to J. Hence, the l.h.s. must be proportional to J as well, which is possible only if $\nu=1/2$. The solution of Eq. (C36) in this case is

$$\kappa\Big|_{\mu_0=0}=\frac{\kappa_0}{6}\left(\theta^{\rm S}\left[\frac{I_0\left(\theta^{\rm S}/4\right)}{I_1\left(\theta^{\rm S}/4\right)}-1\right]-2\right) \tag{C39}$$

and is shown in the inset of Fig. 7(a). Similarly, in the other extreme of $\mu_0=-1$, $\mathsf{C}_0\propto\mathsf{K}$, and so by Eq. (C36), C must be proportional to K, leading to $\kappa=0$.

In the high temperature limit, where Eq. (C37) reduces to

$$6\left(\mathsf{Y}+\left[\mathsf{I}-\mathsf{Y}\right]\mathsf{S}\right)\left(\mathsf{I}-\mathsf{Y}\right)=\theta^{\rm S}\mathsf{Y}, \tag{C40}$$

cf. Eq. (C30). If $\nu = \nu_0$, $\mathsf{Y} = (\mu/\mu_0)\mathsf{I}$, and $\mathsf{S} = \mathsf{S}_0$. As a result, S_0 must be proportional to I, leading to $\nu_0^{\rm FP} = 1/5$, cf. Eq. (C31). Also, $\tilde{p} = 0$ at the fixed point. Thus the analog of Eq. (C34) for the third constraint is given by

$$\mu^{\rm FP} = \left(\sqrt{1 + \left[\frac{\theta^{\rm S}}{6}\right]^2} - \frac{\theta^{\rm S}}{6} \right) \mu_0. \qquad \text{(C41)}$$

Appendix D: Renormalization flows in the elastic moduli space and positive-definiteness of the cavity energy function

Here we consider the renormalization flow on the $(\mu_0, \kappa_0) \mapsto (\mu, \kappa)$ mapping for Eqs. (101), (C26) and (C36). The mappings depend on the dimensionless temperatures: $\theta^{\rm G}$, $\theta^{\rm F}$ and $\theta^{\rm S}$ respectively. Here we assume these three parameters are small, with the aim of obtaining a continuous RG flow. The linearized mapping for Eq. (101) corresponding to constraint (96) can be obtained analytically. For the other two equations, we rearrange them to the form $\mathsf{L}[f_1\,,\, f_2] = 0$, and then Taylor expand near the solution to linearize the mapping and connect small increments of the bare and effective elastic moduli, via

$$\begin{pmatrix} \delta\mu \\ \delta\kappa \end{pmatrix} = N(\mathsf{C}, \mathsf{C}_0, \theta) \begin{pmatrix} \delta\mu_0 \\ \delta\kappa_0 \end{pmatrix}, \qquad \text{(D1)}$$

where the dimensionless stress energy θ is set equal to its values corresponding to the three constraints. The matrix N has the form

$$N = \frac{1}{\Delta} \left(\begin{array}{c|c} \frac{\partial f_1}{\partial \mu_0}\frac{\partial f_2}{\partial \kappa} - \frac{\partial f_1}{\partial \kappa}\frac{\partial f_2}{\partial \mu_0} & \frac{\partial f_1}{\partial \kappa_0}\frac{\partial f_2}{\partial \kappa} - \frac{\partial f_1}{\partial \kappa}\frac{\partial f_2}{\partial \kappa_0} \\ \hline \frac{\partial f_1}{\partial \mu}\frac{\partial f_2}{\partial \mu_0} - \frac{\partial f_1}{\partial \mu_0}\frac{\partial f_2}{\partial \mu} & \frac{\partial f_1}{\partial \mu}\frac{\partial f_2}{\partial \kappa_0} - \frac{\partial f_1}{\partial \kappa_0}\frac{\partial f_2}{\partial \mu} \end{array} \right), \qquad \text{(D2)}$$

$$\Delta = \frac{\partial f_1}{\partial \kappa}\frac{\partial f_2}{\partial \mu} - \frac{\partial f_1}{\partial \mu}\frac{\partial f_2}{\partial \kappa}. \qquad \text{(D3)}$$

The renormalization flows corresponding to constraints Eq. (96) and (98) are shown in Fig. 8 (a) and (b) respectively. The flow for the second constraint, Eq. (97), looks very similar to Fig. 8(a) and is not provided. The renormalization flow clearly reflects the down-renormalization of the elastic constants, discussed in the main text, and leads toward the state with $\mu = \kappa = 0$. This state formally corresponds to an infinitely compressible, uniform liquid.

Finally, we show that the last term in the Eq. (94),

$$\frac{1}{2}\boldsymbol{\varepsilon}^{\rm T}\mathsf{C}\,(\mathsf{C}_0 - \mathsf{C})\,\mathsf{Q}\,\boldsymbol{\varepsilon}^{\rm T}, \qquad \text{(D4)}$$

which describes the cavity contribution to the potential energy of the external load, is always positive. First note that the tensor product in (D4) can be written as

$$\mathsf{C}\,(\mathsf{C}_0 - \mathsf{C})\,\mathsf{Q} = \mathsf{C}_0\mathsf{A}, \qquad \text{(D5)}$$

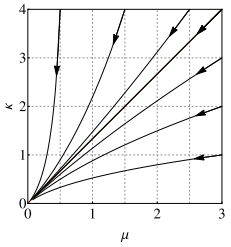

(a)

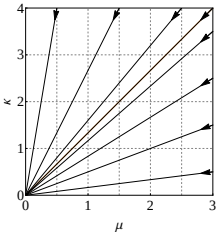

(b)

FIG. 8. Renormalization flow for the $(\mu_0, \kappa_0) \mapsto (\mu, \kappa)$. The respective curvatures of the flow lines have opposite signs in panels (a) and (b). Both flows are calculated for $\theta = 0.1$.

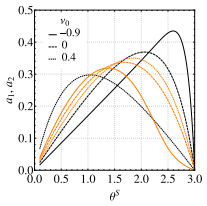

FIG. 9. Coefficients of the tensor A, Eq. (D6) corresponding to the solution of Eq. (101), for several values of the bare Poisson ratio. Black lines correspond to a_1, while the orange lines correspond to a_2, see text for explanation.

where

$$\mathsf{A} = \mathsf{Y}\,(\mathsf{I} - \mathsf{Y})\,(\mathsf{Y} + [\mathsf{I} - \mathsf{Y}]\,\mathsf{S})^{-1} = \mathsf{L}[a_1\,,\, a_2]\,. \qquad \text{(D6)}$$

Since C_0 is positively defined, the sign of (D4) is determined by the sign of the dimensionless coefficients a_1 and a_2. In Fig. 9 we plot them for different values of ν_0, for the constraint from Eq. (96). These coefficients are seen to be positive in the whole parameter range. The corresponding graphs for constraints (97) and (98) are similar and are not shown.

[1] V. Lubchenko and P. G. Wolynes, J. Chem. Phys. **119**, 9088 (2003).
[2] V. Lubchenko and P. G. Wolynes, "Theories of Structural Glass Dynamics: Mosaics, Jamming, and All That," in *Structural Glasses and Supercooled Liquids: Theory, Experiment, and Applications*, edited by P. G. Wolynes and V. Lubchenko (John Wiley & Sons, 2012) pp. 341–379.
[3] F. Mezei and M. Russina, J. Phys. Cond. Mat. **11**, A341 (1999).
[4] Y. Singh, J. P. Stoessel, and P. G. Wolynes, Phys. Rev. Lett. **54**, 1059 (1985).
[5] P. Rabochiy and V. Lubchenko, J. Phys. Chem. B **116**, 5729 (2012).

[6] T. R. Kirkpatrick, D. Thirumalai, and P. G. Wolynes, Phys. Rev. A **40**, 1045 (1989).
[7] X. Xia and P. G. Wolynes, Proc. Natl. Acad. Sci. **97**, 2990 (2000).
[8] V. Lubchenko and P. G. Wolynes, Annu. Rev. Phys. Chem. **58**, 235 (2007).
[9] V. Lubchenko and P. G. Wolynes, Phys. Rev. Lett. **87**, 195901 (2001).
[10] S. Ashtekar, G. Scott, J. Lyding, and M. Gruebele, J. Phys. Chem. Lett. **1**, 1941 (2010).
[11] U. Tracht, M. Wilhelm, A. Heuer, H. Feng, K. Schmidt-Rohr, and H. W. Spiess, Phys. Rev. Lett. **81**, 2727 (1998).
[12] E. V. Russell and N. E. Israeloff, Nature **408**, 695 (2000).
[13] M. T. Cicerone and M. D. Ediger, J. Chem. Phys. **104**, 7210 (1996).
[14] S. Capaccioli, G. Ruocco, and F. Zamponi, J. Phys. Chem. B **112**, 10652 (2008).
[15] P. Rabochiy, P. G. Wolynes, and V. Lubchenko, J. Phys. Chem. B **117**, 15204 (2013).
[16] V. Lubchenko, Proc. Natl. Acad. Sci. **106**, 11506 (2009).
[17] L. Onsager, J. Am. Chem. Soc. **58**, 1486 (1936).
[18] P. Debye, Physik. Z. **13**, 97 (1912).
[19] P. Debye, *Polar molecules* (Dover, 1945).
[20] J. G. Kirkwood, J. Chem. Phys. **7**, 911 (1939).
[21] S. Alexander, Phys. Rep. **296**, 65 (1998).
[22] M. Bienfait, Surf. Sci. **272**, 1 (1972).
[23] H. Taub, G. Torzo, H. J. Lauter, and S. C. Fain Jr., eds., *Phase Transitions in Surface Films 2, NATO ASI Series B*, Vol. 267 (Plenum Press, 1991).
[24] S. Sachdev and D. R. Nelson, Phys. Rev. B **32**, 1480 (1985).
[25] Z. Nussinov, Phys. Rev. B **69**, 014208 (2004).
[26] T. Egami and D. Srolovitz, J. Phys. F: Met. Phys. **12**, 2141 (1982).
[27] D. Srolovitz, K. Maeda, V. Vitek, and T. Egami, Phil. Mag. A **44**, 847 (1981).
[28] H. Mizuno, S. Mossa, and J.-L. Barrat, Europhys. Lett. **104**, 56001 (2013).
[29] D. Bevzenko and V. Lubchenko, J. Phys. Chem. B **113**, 16337 (2009).
[30] L. D. Landau and E. M. Lifshitz, *Theory of Elasticity* (Pergamon Press, 1986).
[31] L. Yan, G. Düring, and M. Wyart, Proc. Natl. Acad. Sci. **110**, 6307 (2013).
[32] H. Yoshino and M. Mézard, Phys. Rev. Lett. **105**, 015504 (2010).
[33] H. Yoshino, J. Chem. Phys. **136**, 214108 (2012).
[34] B. W. H. van Beest, G. J. Kramer, and R. A. van Santen, Phys. Rev. Lett. **64**, 1955 (1990).
[35] E. Flenner, H. Staley, and G. Szamel, Phys. Rev. Lett. **112**, 097801 (2014).
[36] G. Ayton, M. J. P. Gingras, and G. N. Patey, Phys. Rev. Lett. **75**, 2360 (1995).
[37] J. Tomasi and M. Persico, Chem. Rev. **94**, 2027 (1994).
[38] M. Baus and R. Lovett, Phys. Rev. A **44**, 1211 (1991).
[39] C. Teodosiu, *Elastic Models of Crystal Defects* (Springer, 1982).
[40] E. Kröner, Int. J. Sol. Struct. **29**, 1849 (1992).
[41] V. Lubchenko and P. G. Wolynes, Adv. Chem. Phys. **136**, 95 (2007).
[42] A. Zhugayevych and V. Lubchenko, J. Chem. Phys. **132**, 044508 (2010).
[43] A. Zhugayevych and V. Lubchenko, J. Chem. Phys. **133**, 234503 (2010).
[44] A. Zhugayevych and V. Lubchenko, J. Chem. Phys. **133**, 234504 (2010).
[45] C. Cammarota and G. Biroli, Europhys. Lett. **98**, 36005 (2012).
[46] D. K. Biegelsen and R. A. Street, Phys. Rev. Lett. **44**, 803 (1980).
[47] M. A. Bösch and J. Shah, Phys. Rev. Lett. **42**, 118 (1979).
[48] S. Corezzi, S. Caponi, F. Rossi, and D. Fioretto, J. Phys. Chem. B **117**, 14477 (2013).
[49] F. Léonforte, A. Tanguy, J. P. Wittmer, and J.-L. Barrat, Phys. Rev. Lett. **97**, 055501 (2006).
[50] A. Paul, S. Sengupta, and M. Rao, J. Phys.: Condens. Matter **26**, 015007 (2014).
[51] H. Wagner, D. Bedorf, S. Kchemann, M. Schwabe, Z. Bo, W. Arnold, and K. Samwer, Nature Materials **10**, 439 (2011).
[52] S. G. Mayr, Phys. Rev. B **79**, 060201 (2009).
[53] W. Schirmacher, Europhys. Lett. **73**, 892 (2006).
[54] A. Marruzzo, W. Schirmacher, A. Fratalocchi, and G. Ruocco, Sci. Rep. **3**, 1407 (2013).
[55] E. Kröner, Arch. Ration. Mech. Anal. **4**, 18 (1960).
[56] P. Dederichs, C. Lehmann, H. Schober, A. Scholz, and R. Zeller, J. Nucl. Mat. **69-70**, 176 (1978).
[57] M. P. Puls, *The Effect of Hydrogen and Hydrides on the Integrity of Zirconium Alloy Components: Delayed Hydride Cracking* (Springer, 2012).
[58] L. D. Landau and E. M. Lifshitz, *Electrodynamics of Continuous Media* (Pergamon Press, 1960).
[59] J. D. Jackson, *Classical Electrodynamics* (Wiley, 1975).
[60] E. Kröner, in *Theory of Crystal Defects. Proc. of the Summer school held in Hrazany in September 1964* (Academic Press, 1966).
[61] L. J. Walpole, Adv. App. Mech. **21**, 169 (1981).
[62] M. Mezard, G. Parisi, and M. Virasoro, *Spin Glass Theory And Beyond* (World Scientific, 1987).
[63] T. R. Kirkpatrick and P. G. Wolynes, Phys. Rev. B **36**, 8552 (1987).
[64] M. Mézard and G. Parisi, J. Chem. Phys. **111**, 1076 (1999).
[65] T. R. Kirkpatrick and P. G. Wolynes, Phys. Rev. A **35**, 3072 (1987).
[66] J. Kurchan, G. Parisi, P. Urbani, and F. Zamponi, J. Phys. Chem. B **117**, 12979 (2013).
[67] P. G. Wolynes and V. Lubchenko, eds., *Structural Glasses and Supercooled Liquids: Theory, Experiment, and Applications* (John Wiley & Sons, 2012) pp. 341–379.
[68] D. J. Bacon, D. M. Barnett, and R. O. Scattergood, Prog. Mater Sci. **23**, 51 (1979).
[69] T. Mura, *Micromechanics of Defects in Solids* (Martinus Nijhoff, 1987).
[70] W. Känzig, J. Phys. Chem. Solids **23**, 479 (1962).
[71] A. Nowick and W. Heller, Adv. Phys. **12**, 251 (1963).
[72] A. Loidl, Annu. Rev. Phys. Chem. **40**, 29 (1989).
[73] R. M. Lynden-Bell and K. H. Michel, Rev. Mod. Phys. **66**, 721 (1994).
[74] J. D. Eshelby, Phil. Trans. Roy. Soc. A **244**, 87 (1951).
[75] J. D. Eshelby, Proc. Roy. Soc. A **241**, 376 (1957).
[76] H. L. Friedman, Molecular Physics **29**, 1533 (1975).
[77] M. M. Mehrabadi and S. C. Cowin, Q. J. Mech. Appl. Math. **43**, 15 (1990).
[78] J. P. Stoessel and P. G. Wolynes, J. Chem. Phys. **80**, 4502 (1984).
[79] M. Baus and J.-L. Colot, J. Phys. C: Solid State Phys. **19**, L135 (1986).
[80] H. Lowen, J. Phys.: Condens. Matter **2**, 8477 (1990).
[81] P. Rabochiy and V. Lubchenko, J. Chem. Phys. **136**, 084504 (2012).
[82] S. M. Sharma and S. Sikka, Prog. Mater. Sci. **40**, 1 (1996).
[83] V. V. Brazhkin and A. G. Lyapin, J. Phys. Cond. Mat. **15**, 6059 (2003).
[84] E. Ponyatovsky and O. Barkalov, Mat. Sci. Rep. **8**, 147 (1992).
[85] R. J. Hemley, A. P. Jephcoat, H. K. Mao, L. C. Ming, and M. H. Manghnani, Nature **334**, 52 (1988).
[86] G. Parisi and F. Zamponi, Rev. Mod. Phys. **82**, 789 (2010).
[87] T. S. Grigera, V. Martin-Mayor, G. Parisi, and P. Verrocchio, Nature **422**, 289 (2003).
[88] A. C. Anderson, in *Amorphous Solids: Low-Temperature Properties*, edited by W. A. Phillips (Springer-Verlag, Berlin, Heidelberg, New York, 1981).
[89] Y. P. Joshi, Phys. Stat. Sol. (b) **95**, 317 (1979).
[90] V. Lubchenko and P. G. Wolynes, Proc. Natl. Acad. Sci. **100**, 1515 (2003).
[91] W. A. Phillips, ed., *Amorphous Solids: Low-Temperature Properties* (Springer-Verlag, Berlin, Heidelberg, New York, 1981).
[92] J. Qu and M. Cherkaoui, *Fundamentals of Micromechanics of*

Solids (John Wiley & Sons, Inc., 2006).
[93] A. Abramowitz and I. Stegun, eds., *Handbook of Mathematical Functions* (Dover, 1964).
[94] G. Mussardo, *Statistical Field Theory: An Introduction to Exactly Solved Models in Statistical Physics* (Oxford University Press, 2010).